Settling of small particles near vortices and in turbulence

By J. DÁVILA† AND J. C. R. HUNT‡

Department of Applied Mathematics and Theoretical Physics, University of Cambridge,
Silver Street, Cambridge CB3 9EW, UK

The trajectories of small heavy particles in a gravitational field, having fall speed in still fluid $\tilde{V}_T$ and moving with velocity $\tilde{V}$ near fixed line vortices with radius $\tilde{R}_v$ and circulation $\tilde{\Gamma}$, are determined by a balance between the settling process and the centrifugal effects of the particles' inertia. We show that the main characteristics are determined by two parameters: the dimensionless ratio $V_T = \tilde{V}_T \tilde{R}_v / \tilde{\Gamma}$ and a new parameter (F_p) given by the ratio between the relaxation time of the particle ($\tilde{t}_p$) and the time ($\tilde{\Gamma}/\tilde{V}_T^2$) for the particle to move around a vortex when V_T is of order unity or small.

The average time $\Delta\tilde{T}$ for particles to settle between two levels a distance $\tilde{Y}_0$ above and below the vortex (where $\tilde{Y}_0 \gg \tilde{\Gamma}/\tilde{V}_T$) and the average vertical velocity of particles $\langle\tilde{V}_y\rangle_L$ along their trajectories depends on the dimensionless parameters V_T and F_p. The bulk settling velocity $\langle\tilde{V}_y\rangle_B = 2\tilde{Y}_0/\langle\Delta\tilde{T}\rangle$, where the average value of $\langle\Delta\tilde{T}\rangle$ is taken over all initial particle positions of the upper level, is only equal to $\langle\tilde{V}_y\rangle_L$ for small values of the effective volume fraction within which the trajectories of the particles are distorted, $\alpha = (\tilde{\Gamma}/\tilde{V}_T)^2/\tilde{Y}_0^2$. It is shown here how $\langle\tilde{V}_y\rangle_B$ is related to $\Delta\tilde{\eta}(\tilde{X}_0)$, the difference between the vertical settling distances with and without the vortex for particles starting on $(\tilde{X}_0, \tilde{Y}_0)$ and falling for a fixed period $\Delta\tilde{T}_T \gg \tilde{\Gamma}/\tilde{V}_T^2$; $\langle\tilde{V}_y\rangle_B = \tilde{V}_T[1 - \alpha D]$, where $D = \int_{-\infty}^{\infty}(\Delta\tilde{\eta}\,d\tilde{X}_0/(\tilde{\Gamma}/\tilde{V}_T)^2)$ is the drift integral. The maximum value of $\langle\tilde{V}_y\rangle_B$ for any constant value of V_T occurs when $F_p = F_{p_M} \sim 1$ and the minimum when $F_p = F_{p_m} > F_{p_M}$, where typically $3 < F_{p_m} < 5$.

Individual trajectories and the bulk quantities D and $\tilde{V}_y\rangle_B$ have been calculated analytically in two limits, first $F_p \to 0$, finite V_T, and secondly $V_T \gg 1$. They have also been computed for the range $0 < F_p < 10^2$, $0 < V_T < 5$ in the case of a Rankine vortex. The results of this study are consistent with experimental observations of the pattern of particle motion and on how the fall speed of inertial particles in turbulent flows (where the vorticity is concentrated in small regions) is typically up to 80% greater than in still fluid for inertial particles ($F_p \sim 1$) whose terminal velocity is less than the root mean square of the fluid velocity, $\tilde{u}'$, and typically up to 20% less for particles with a terminal velocity larger than $\tilde{u}'$. If $\tilde{V}_T/\tilde{u}' > 4$ the differences are negligible.

1. Introduction

Recent theoretical studies have shown how the trajectories of small dense or buoyant particles in fluid flows induced by steady vortices of strength $\tilde{\Gamma}$ (with a typical radius

---

† Also at: Grupo de Mecánica de Fluidos, University of Seville, Spain
‡ Present address: Departments of Space and Climate Physics and Geological Sciences, University College, Gower Street, London WC1E 6BT, UK

$\tilde{R}_v$ and maximum velocity $\tilde{U} = \tilde{\Gamma}/\tilde{R}_v$) have many interesting and even unexpected forms (e.g. Maxey & Corrsin 1986; Maxey 1987; McLaughlin 1988; Gañán-Calvo & Lasheras 1991). These depend sensitively on the ratio (β) of the density of the particles ($\tilde{\rho}_p$) to that of the fluid ($\tilde{\rho}_f$), the Reynolds number based on the relative particle motion (Re), and on the ratios of the inertial forces in the fluid, as generated by the vortices, to the buoyancy and drag forces acting on the particles. The latter are defined by two non-dimensional numbers, namely the Froude number of the flow $F_f = \tilde{U}^2/(\tilde{g}\tilde{R}_v)$, where $\tilde{g}$ is the acceleration due to gravity, and the Stokes number $St = \tilde{t}_p\tilde{U}/\tilde{R}_v$, where $\tilde{t}_p$ $[= (\beta - 1)\tilde{d}_p^2/(18\tilde{v})$ for small particles of diameter $\tilde{d}_p$ in a fluid of kinematic viscosity $\tilde{v}]$ is the viscous relaxation time of the particle. For particles moving under gravity, $\tilde{t}_p = \tilde{V}_T/\tilde{g}$ and $St = \tilde{U}\tilde{V}_T/(\tilde{g}\tilde{R}_v)$.

Depending on whether β is less or greater than one, particles are accelerated towards or away from the vortices. Also the pattern of motion is quite different depending on whether the terminal velocity $\tilde{V}_T$ is large or small compared with $\tilde{U}$. If it is small (or $V_T = St/F_f \ll 1$) and if the inertia is locally small enough, the points where the motion of the particles are arrested are also equilibrium points (in the sense that particles could remain there at rest). As with other nonlinear dynamical systems, general features of particle trajectories can be derived by studying their form near the equilibrium points of the system (Raju & Meiburg 1997). This approach is applied here to the important environmental and engineering problem of understanding and estimating the bulk movement and settling velocities of particles near vortices. We particularly focus some of our calculations on a parameter range, corresponding to small solid particles settling in gases, where $\beta \gg 1$ and $Re_T = \tilde{d}_p\tilde{V}_T/\tilde{v} < 1$ (see Appendix A). However, some of the results are applicable in other parameter ranges, such as those corresponding to heavy particles in liquids. Usually, these features are defined in terms of the Stokes number St or its inverse, and the settling velocity in fluid at rest relative to the flow speed V_T or the Froude number F_f (see e.g. Maxey & Corrsin 1986; Chein & Chung 1987; Wen *et al.* 1992; Martin & Meiburg 1994). However, these dimensionless groups must be modified in order to quantify and understand the motion of particles near the vortices and especially near the equilibrium points because here the characteristic time seen by the particles $\tilde{t}_c$ is not the residence time of the fluid particles $\tilde{t}_r = \tilde{\Gamma}_v/\tilde{U}^2$. It is necessary to introduce a modified non-dimensional Froude number of the particle (see table 1) which is the ratio of the inertial forces experienced *by a particle* to the buoyancy forces. We refer to this as the particle Froude number $F_p = \tilde{V}_T^3/(\tilde{g}\,\tilde{\Gamma})(= St^3/F_f^2)$. It is also equal to the ratio of the distance taken by a particle to reach its terminal velocity ($\tilde{V}_T\tilde{t}_p$) to the minimum radius of particle trajectories around the vortex ($\tilde{\Gamma}/\tilde{V}_T$).

In order to quantify the characteristic features of the particles' trajectories in complex flows we must clarify some of the usual measures. We focus here on settling times and settling velocities. The trajectories in figure 1 show why, if a solid particle falls from a plane (say $\tilde{y} = \tilde{Y}_0$) well above a vortex to another ($\tilde{y} = \tilde{Y}_1$) well below the vortex, the time it takes, $\Delta\tilde{T}$, differs from the terminal fall time $\Delta\tilde{T}_T$ it takes in the still fluid, where $\Delta\tilde{T}_T = (\tilde{Y}_0 - \tilde{Y}_1)/\tilde{V}_T$. An equivalent way to define this difference in the settling of particles with and without a vortex is in terms of the level that a particle reaches (say $\tilde{Y} = \tilde{Y}_1 + \Delta\tilde{\eta}$) in a certain time (say $\Delta\tilde{T}_T$). If $|\tilde{Y}_1|$ is large enough, when $|\tilde{Y}|$ is large $\tilde{V}_y \simeq -\tilde{V}_T$ and therefore $\Delta\tilde{T} = (\tilde{Y}_0 - \tilde{Y}_1 + \Delta\tilde{\eta})/\tilde{V}_T$. Hence, $\Delta\tilde{\eta} = \tilde{V}_T(\Delta\tilde{T} - \Delta\tilde{T}_T)$.

Previous studies of velocity statistics of settling particles have focused on different averages of the settling velocity. The first definition is the Eulerian average velocity

Description	Symbol	Definition	Comment
Density ratio	β	$\dfrac{\tilde{\rho}_p}{\tilde{\rho}_f}$	$\beta \gg 1$ for aerosol particles
Flow Froude number	F_f	$\dfrac{\tilde{U}^3}{\tilde{g}\,\tilde{\Gamma}} = \dfrac{\tilde{\Gamma}^2}{\tilde{g}\,\tilde{R}^3}$	$\dfrac{\text{Fluid inertia}}{\text{Buoyancy forces}}$
Stokes number	St	$\tilde{t}_p \dfrac{\tilde{U}^2}{\tilde{\Gamma}}$	$\dfrac{\text{Particle inertia}}{\text{Drag forces}}$ if $\tilde{t}_c \sim \tilde{t}_r$
Dimensionless terminal velocity	V_T	$\dfrac{\tilde{V}_T}{\tilde{U}} = \dfrac{St}{F_f}$	It determines the position of the equilibrium points
Particle Froude number	F_p	$\dfrac{\tilde{V}_T^3}{\tilde{g}\,\tilde{\Gamma}} = \tilde{t}_p \dfrac{\tilde{V}_T^2}{\tilde{\Gamma}} = V_T^2 St$	$\dfrac{\text{Particle inertia}}{\text{Buoyancy forces}}$
Flow/particle Reynolds number	Re_p	$\dfrac{\tilde{d}_p \tilde{U}}{\tilde{v}}$	Meaningful if the relative velocity $\sim \tilde{U}$
Terminal/particle Reynolds number	Re_T	$\dfrac{\tilde{d}_p \tilde{V}_T}{\tilde{v}}$	See Appendix A

TABLE 1. Dimensionless ratios for the dynamics of particles near a vortex.
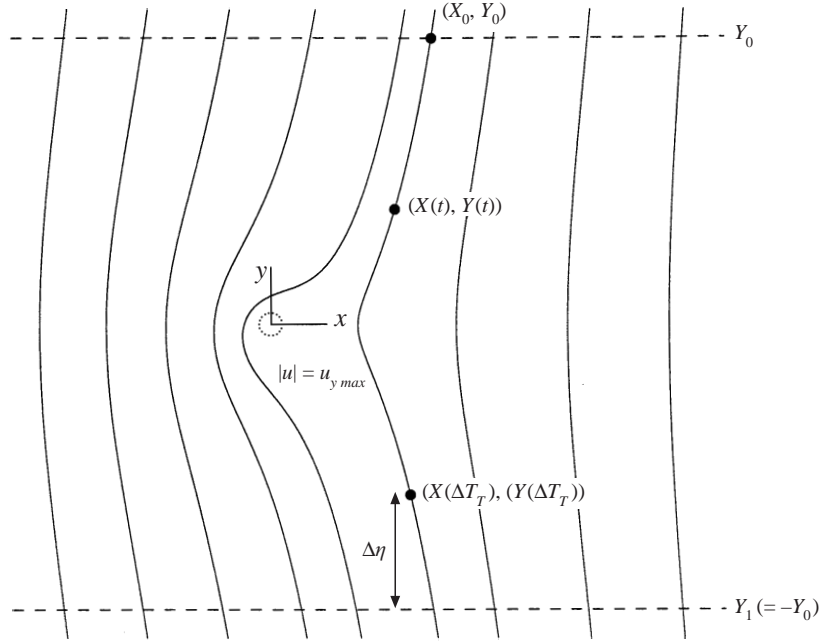

FIGURE 1. Schematic diagram of the coordinates $(\tilde{x}, \tilde{y})$ relative to the centre of the vortex and trajectories $(\tilde{X}(t), \tilde{Y}(t))$ of particles moving over a period $\Delta\tilde{T}_T$ from a plane $\tilde{Y} = \tilde{Y}_0$. In the absence of the vortex $\tilde{Y}(\Delta\tilde{T}_T) = \tilde{Y}_0 - \tilde{V}_T \Delta\tilde{T}_T = -\tilde{Y}_0$ and with the vortex $\tilde{Y}(\Delta\tilde{T}_T) = \tilde{Y}_0 + \Delta\tilde{Y} = \tilde{Y}_1 + \Delta\tilde{\eta}$.

at $\tilde{x}$, $\langle \tilde{V}_y \rangle_E$, i.e. the average of the vertical velocity of particles at a particular point, $\tilde{V}_y(\tilde{x}, \tilde{y}, \tilde{t})$, weighted by the particles' concentration distribution $p(\tilde{x}, \tilde{y}, \tilde{t})$. In homogeneous turbulence with a statistically homogeneous distribution of particles, $\langle \tilde{V}_y \rangle_E$ is also equal to the spatial average. The second definition is the Lagrangian

average settling velocity,

$$\langle \tilde{V}_y \rangle_L = \left\langle \frac{1}{\Delta \tilde{T}_T} \int_{\tilde{t}=0}^{\tilde{t}=\Delta \tilde{T}_T} \tilde{V}_y(\tilde{X}, \tilde{Y}; \tilde{X}_0) \, \mathrm{d}\tilde{t} \right\rangle = \left\langle \frac{\tilde{Y}_0 - \tilde{Y}(\tilde{X}_0, \Delta \tilde{T}_T)}{\Delta \tilde{T}_T} \right\rangle$$

$$= \tilde{V}_T - \frac{\langle \Delta \tilde{\eta}(\tilde{X}_0, \Delta \tilde{T}_T) \rangle}{\Delta \tilde{T}_T}, \tag{1.1}$$

where $\tilde{Y}(\tilde{X}_0, \Delta \tilde{T}_T)$ is the level of a particle at time $\Delta \tilde{T}_T$. Here, the average has been taken over an ensemble of particles such as those having different starting positions; other different ensembles could be defined leading to different values of $\langle \tilde{V}_y \rangle_L$. The third definition, often used in engineering, is the bulk settling velocity, $\langle \tilde{V}_y \rangle_B = (\tilde{Y}_0 - \tilde{Y}_1)/\langle \Delta \tilde{T} \rangle$. For large values of $|\tilde{Y}_1|$

$$\langle \tilde{V}_y \rangle_B = \frac{\tilde{V}_T}{\langle 1 + \Delta \tilde{\eta}/(\tilde{Y}_0 - \tilde{Y}_1) \rangle}. \tag{1.2}$$

Comparing the second and third definitions shows that the mean Lagrangian velocity $\langle \tilde{V}_y \rangle_L$ is more weighted by trajectories of particles with high velocities, whereas the bulk settling velocity is more weighted by slow particles. The distinction between 'bulk' properties of two-phase flows and spatially averaged quantities defined in the fluid phase of the flow, such as pressure gradients, was pointed out by Kowe *et al.* (1988).

In the special case of a homogeneous velocity field with no mean vertical velocity (i.e. $\langle \tilde{u}_y \rangle_E = 0$), if the particle distribution is (artificially) uniform, Maxey & Corrsin (1986) showed that for particles unaffected by inertia forces (i.e. $St \to 0$) $\langle \tilde{V}_y \rangle_E = \langle \tilde{V}_y \rangle_L = \tilde{V}_T$ (an Eulerian result). In most other cases $\langle \tilde{V}_y \rangle_L$ does not equal $\langle \tilde{V}_y \rangle_E$ and neither $\langle \tilde{V}_y \rangle_L$ nor $\langle \tilde{V}_y \rangle_B$ equals $\tilde{V}_T$. When the inertia of the particle is small enough ($St \to 0$) and $\tilde{V}_T$ is significantly smaller than the smallest scale fluctuations of the fluid velocity, the particle trajectories differ only slightly from those of fluid particles (e.g. Wang & Stock 1993; Hunt, Perkins & Fung 1994). However, in the other limit, where $\tilde{V}_T$ is much larger than the root mean square of the vertical velocity component of the flow field $\tilde{u}'_y$ so that the particle passes through the turbulence as its falls, then $\langle \tilde{V}_y \rangle_B$ is less than $\tilde{V}_T$ by an amount of the order of $\tilde{u}'^2_y/\tilde{V}_T$ (see Appendix B). In the usual situation when $\tilde{V}_T$ is of the order $\tilde{u}'_y$ and $St \neq 0$, and when the particle concentration is not uniform across the flow, no simple generalization is possible; different results have been obtained in different calculations based on differing assumptions. Maxey & Corrsin (1986) and Maxey (1987) found that $\langle \tilde{V}_y \rangle_E > \tilde{V}_T$ in randomly orientated cellular flows and numerically simulated homogeneous turbulent flows. Wang & Maxey (1993), who suggested that there are strong similarities in the settling motion of particles in these two types of flow, showed that $\langle \tilde{V}_y \rangle_L > \tilde{V}_T$. However, Fung (1993) found that $\langle \tilde{V}_y \rangle_B < \tilde{V}_T$, where $\tilde{V}_T \sim \tilde{u}'_y$, in a given random velocity field simulating that of turbulence. In this paper, we show that such differences can be explained by differences in the definition of $\langle \tilde{V}_y \rangle_E$, $\langle \tilde{V}_y \rangle_L$ and $\langle \tilde{V}_y \rangle_B$ and the variation in the initial concentration of particles in certain regions of the flow fields, as well as by physical parameters, such as $\tilde{V}_T/\tilde{u}'_0$.

In §2, we present the equation of motion and some properties of the equilibrium points for particles moving near line vortices. In §3, we derive the asymptotic equations for particles whose inertia is negligible when settling in a vortex flow. Some of the singular features of the trajectories of particles are discussed in §4. In §5, we calculate the differential settling distance $\tilde{Y} - \tilde{Y}_1$ for different values of V_T and F_p in the

flow field near vortices and thence derive the average settling velocities (§6). These results help to explain previously published results about different flow fields and provide general physical concepts to describe the settling and transport of particles in turbulent flows. We show that our results of settling around vortices are consistent with those of the recent experiments of Srdic (1999) for particles sedimenting in homogeneous turbulence. Other conclusions of this work are given in §7.

2. Equations for the dynamics and trajectories of small particles moving near vortices

To non-dimensionalize our equations, we scale the dimensional variables using the maximum vertical velocity of the fluid, $\tilde{U}$, and the characteristic circulation of the vortices, $\tilde{\Gamma}$. The lengthscales are effectively normalized on the radius of the vortex $\tilde{R}_v = \tilde{\Gamma}/\tilde{U}$. As explained in §1, the relative order of magnitude of the particle inertia to the combined effect of buoyancy and drag forces is proportional to the Stokes number

$$St = \frac{(\beta - 1)}{k_T} \frac{\tilde{d}_p^2}{18\tilde{v}} \frac{\tilde{U}^2}{\tilde{\Gamma}}, \tag{2.1}$$

St is effectively the ratio between two characteristic times: the characteristic viscous response time of the particle,

$$\tilde{t}_p = \frac{\tilde{V}_T}{\tilde{g}} = \frac{(\beta - 1)}{k_T} \frac{\tilde{d}_p^2}{18\,\tilde{v}}, $$

and the residence time for the change of the fluid velocity seen by a *fluid particle* $\tilde{t}_r = \tilde{\Gamma}/\tilde{U}^2$. Since the timescale of change of velocity seen by the particles can significantly differ from $\tilde{\Gamma}/\tilde{U}^2$, a modified parameter is introduced in §3 to represent the importance of the inertia of particles moving around vortex tubes or moving far away from any vorticity region. In this paper, we assume that the Reynolds number of the particles based on their relative motion $\tilde{V}_{rel} = |\tilde{V} - \tilde{u}|$, i.e. $Re_p = \tilde{V}_{rel}\tilde{d}_p/\tilde{v}$, is small. To consider finite values of the particle Reynolds number we introduce k_T, the ratio between the actual drag force and the Stokes drag, defined for $Re_p = 0$. This allows us to assume a linear relation between drag and V_{rel} when $Re_T = |\tilde{V}_T|\tilde{d}_p/\tilde{v} < 1$ (see Appendix A). The buoyancy forces acting on the particles can be expressed in terms of the dimensionless terminal velocity V_T. This is related to St and the fluid Froude number, $F_f = \tilde{U}^3/\tilde{g}\tilde{\Gamma}$, by the usual relationship $V_T = St/F_f$. The fluid Froude number does not depend on the particle size, but on properties of the fluid flow and on the acceleration of the gravity, $\tilde{g}$.

The equations which determine the instantaneous position, X, and velocity, V, of a small spherical particle when $Re_T < 1$ are given, in dimensionless form, by (Maxey & Riley 1983; Magnaudet & Eames 2000)

$$\frac{dX}{dt} = V, \tag{2.2a}$$

$$\frac{dV}{dt} = \frac{\beta - 1}{\beta + C_M} \frac{1}{St}(V_T + u - V) + \frac{1 + C_M}{\beta + C_M} \frac{Du}{Dt}, \tag{2.2b}$$

where d/dt is the derivative following the particle, D/Dt is the derivative following the fluid, C_M is the added-mass coefficient (equal to $\frac{1}{2}$), and u is the velocity of the
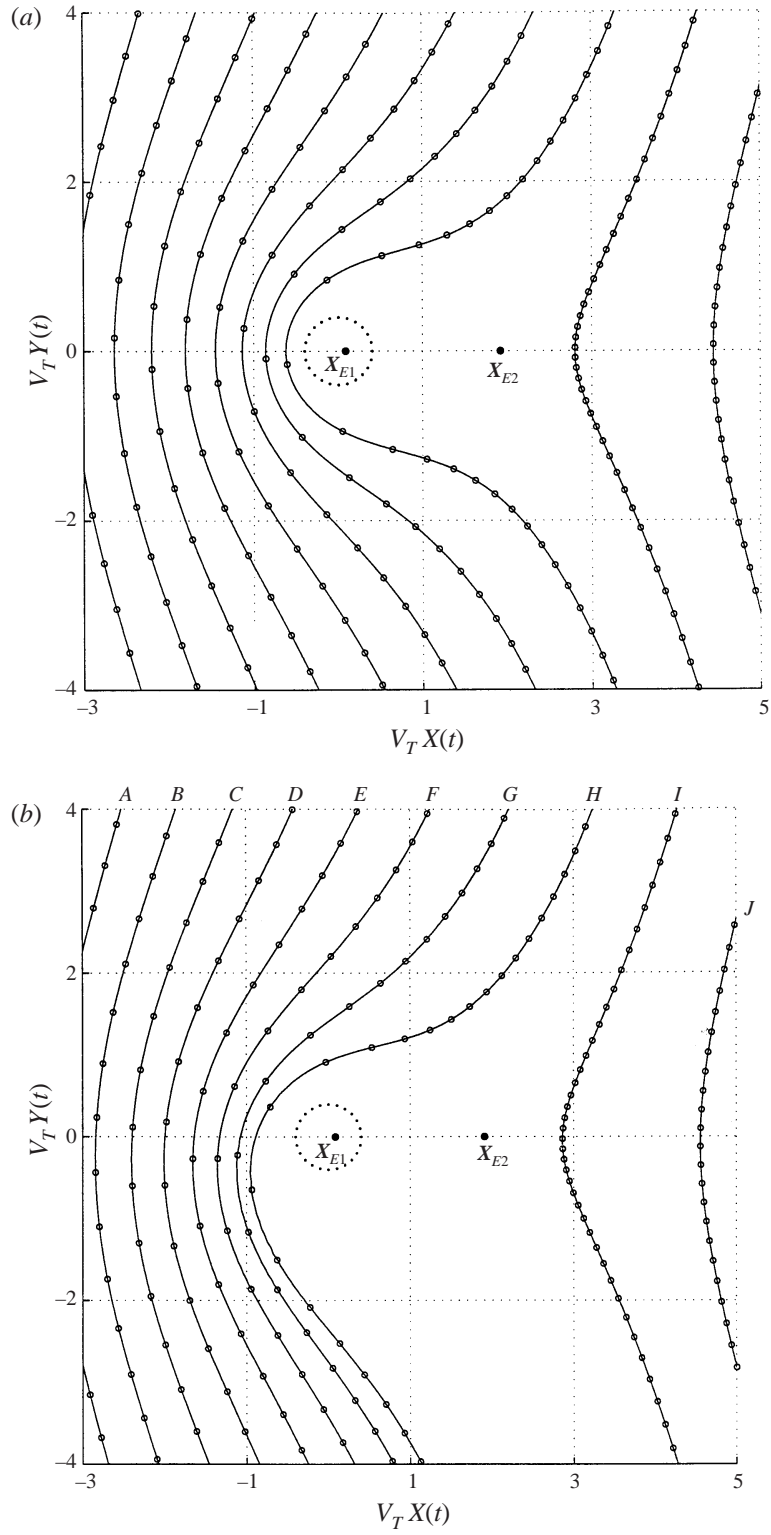
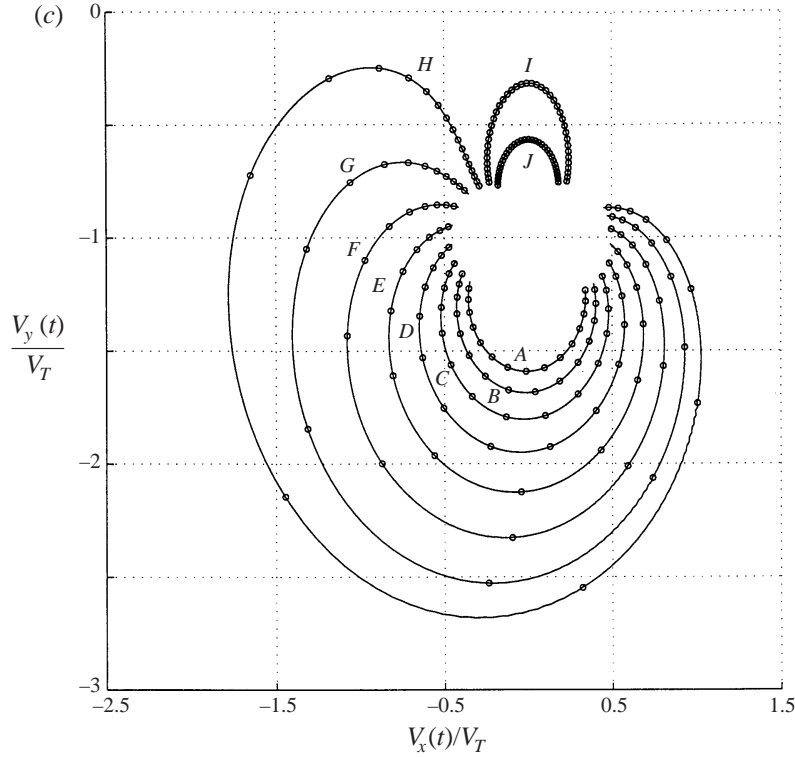FIGURE 2(*a,b*). For caption see facing page.

FIGURE 2. (*a*) Normalized trajectories of non-inertial particles $(X(t), Y(t))$ for $St = 0$ and $V_T = 0.4$. The position of the node (X_{E1}) and the saddle point (X_{E2}) of the system (2.2) for these values of St and V_T is shown. The elapsed time interval between the tick marks was $\Delta t = 0.4/V_T^2$. Also dotted circle with radius $r = 1$ is shown as reference. (*b*) Normalized trajectories of inertial particles $(X(t), Y(t))$ for $St = 1.0$ and $V_T = 0.4$ ($F_p = 0.16$). The position of the unstable focus (X_{E1}) and the saddle point (X_{E2}) of the system (2.2) for these values of St and V_T is shown. The elapsed time interval between the tick marks was $\Delta t = 0.4/V_T^2$. Also dotted circle with radius $r = 1$ is shown as reference. (*c*) Velocity phase plane (V_x, V_y) for the same particles as in (*b*). The capital letters indicate the correspondence with the trajectories of (*b*). Note that the tick marks also correspond to those of (*b*).

undisturbed fluid at X. In these equations it is also assumed that the particle diameter is much less than the characteristic length of the fluid flow, i.e.

$$d_p \ll \frac{\|\nabla \boldsymbol{u}\|}{\|\nabla \nabla \boldsymbol{u}\|}. \tag{2.3}$$

Equation (2.2*b*) is valid for small particles in fluids where the only important forces are gravity, drag, and particle and fluid inertia. Lift and history effects have been neglected.

For all the cases examined here, the initial condition at the position X_0 is the simplest possible, namely that the particles are in equilibrium with the surrounding flow conditions:

$$X(t = 0) = X_0,$$
$$V(t = 0) = \boldsymbol{u}(X_0, t = 0) + V_T. \tag{2.4}$$

Thus, if $\boldsymbol{u}$ were constant, V would not change. Since the characteristic response time of the particle to the flow conditions ($\tilde{t}_p$) is much smaller than the time it takes to reach

the vortex, the influence of the initial conditions can be neglected. The trajectories of particles were obtained by integrating the system of ordinary differential equations (2.2) corresponding to the x- and y-components of the vectors, using a variable-order variable-step size Runge–Kutta method (Press *et al.* 1992).

In order to show the main features of the dynamics of heavy particles moving in vortex flows, we consider the Rankine vortex, defined by a smooth transition from solid rotation close to its centre to an irrotational 'free-vortex' flow field from it. The normalized velocity field in Cartesian coordinates is given by

$$\boldsymbol{u} = (u_x, u_y) = \left(\frac{-2y}{1 + x^2 + y^2}, \frac{2x}{1 + x^2 + y^2} \right), \tag{2.5}$$

so that the maximum value of the velocity $|\boldsymbol{u}| = 1$ is given on the unit circle. For the falling particle $\boldsymbol{V}_T = (0, -V_T)$, where the Y-axis is anti-parallel to the direction of gravity (without loss of generality). To simplify the problem, we have studied the case of aerosol particles $\beta \gg 1$. Then (2.2b) can be substituted by

$$\frac{\mathrm{d}\boldsymbol{V}}{\mathrm{d}t} = \frac{1}{St}(\boldsymbol{V}_T + \boldsymbol{u} - \boldsymbol{V}). \tag{2.6}$$

In figure 2(a), we have first plotted the trajectories of non-inertial aerosol particles with $St = 0$ and $V_T = 0.4$, and then in figure 2(b), those of inertial aerosol particles with $St = 1.0$ and $V_T = 0.4$, calculated using (2.5) and (2.6). In the limit of zero Stokes number, the trajectories are symmetric about $y = 0$ and some particles follow closed trajectories around the centre of the vortex. When $St > 0$, as first demonstrated for cellular flows by Maxey & Corrsin (1986), closed trajectories do not exist. Because of the centrifugal inertial force, particles released inside the vortex gradually drift outward on a timescale $t = f(V_T)/F_f$, where $f(V_T)$ is a function of the dimensionless terminal velocity (Perkins & Hunt 1987). In figure 2(c), we have plotted the instantaneous horizontal and vertical velocity of particles for the same trajectories and values of the dimensionless parameters chosen in figure 2(b).

The equilibrium points of the system (2.2), where $\mathrm{d}\boldsymbol{X}/\mathrm{d}t = \mathrm{d}^2\boldsymbol{X}/\mathrm{d}t^2 = 0$, are defined as $\boldsymbol{X}_E = (X_E, Y_E)$. The position of the equilibrium points in an irrotational vortex for any value of the density ratio β and the parameter V_T has been obtained by Raju & Meiburg (1997). We have concentrated on the case $\beta \gg 1$. Therefore, at these points,

$$\boldsymbol{u}(\boldsymbol{X}_E) + \boldsymbol{V}_T = 0. \tag{2.7}$$

We consider the displacement of inertial particles near these equilibrium points, noting that only when $St \to 0$ do the particles reach equilibrium at these points, as shown later. When the inertia of the particles is small, (2.7) is valid even when $\beta \sim 1$.

For the Rankine vortex (with maximum normalized velocity $|\boldsymbol{u}| = 1$), (2.7) has two real solutions if $V_T < 1$ and no solution if $V_T > 1$, namely

$$X_{E1} = \frac{1 - \sqrt{1 - V_T^2}}{V_T}, \quad Y_{E1} = 0, \quad X_{E2} = \frac{1 + \sqrt{1 - V_T^2}}{V_T}, \quad Y_{E2} = 0. \tag{2.8}$$

As $V_T \to 0$, $\boldsymbol{X}_{E1} \to (0, 0)$, while $\boldsymbol{X}_{E2}$ tends to $(2/V_T, 0)$. Hence, the characteristic length-scale over which the particle trajectory changes is $1/V_T$, or in dimensional terms $\tilde{\Gamma}/\tilde{V}_T$. $\boldsymbol{X}_{E1}$ is a focus (unstable if $St > 0$, i.e. $\beta > 1$) and $\boldsymbol{X}_{E2}$ is a saddle point. The position of these points are shown in figures 2(a) and 2(b). Similar results for a Burgers vortex were obtained by Marcu, Meiburg & Newton (1995). They showed

that when there is a small strain on the vortex, the trajectories of the particles change far from the vortex core and a third equilibrium point (stable node) appears.

3. Asymptotic analysis for particles of small inertia

3.1. *Heavy particles with small inertia along their whole trajectory*

When the fall speed V_T is small or of order unity and if the inertia is small enough, as heavy particles react to the changes in the flow, their trajectories are modified by the vortices over regions where the fluid velocity $|\boldsymbol{u}| \sim V_T$. Their velocities are such that $|\boldsymbol{V}| \sim V_T$, as shown in figure 2($c$), an estimate consistent with the results given in the previous section. We showed that for small values of V_T there is a saddle point at a distance from the origin of the vortex of the order $1/V_T$. Since in the Rankine vortex (outside the core) the fluid velocity decays as $1/|\boldsymbol{x}|$, the fluid velocities are of the order V_T. It follows that the timescale for particle motion in this region is $t \sim 1/V_T^2$. The same argument can be used for other vortical flows which decay more slowly with radius, in proportion to $1/|\boldsymbol{x}|^a$. (A value of $a < 1$ but close to one is usually measured in three-dimensional vortex tubes, a being the parameter that determines the critical Squires number for the vortex breakdown; Fernández-Feria, Fernández de la Mora & Barrero 1995). Hence, the appropriate dimensionless variables to be used for this problem are

$$\left. \begin{aligned} \hat{\boldsymbol{V}} &= \frac{\tilde{\boldsymbol{V}}}{\tilde{V}_T} = \frac{\boldsymbol{V}}{V_T}, && \hat{\boldsymbol{u}} = \frac{\tilde{\boldsymbol{u}}}{\tilde{V}_T} = \frac{\boldsymbol{u}}{V_T}, \\ \hat{\boldsymbol{X}} &= \frac{\tilde{\boldsymbol{X}}}{\tilde{\Gamma}/(\tilde{V}_T \tilde{U}^{a-1})^{1/a}} = V_T^{1/a} \boldsymbol{X}, && \hat{t} = \frac{\tilde{t}}{\tilde{\Gamma}/(\tilde{V}_T^{a+1} \tilde{U}^{a-1})^{1/a}} = V_T^{(1+1/a)} t. \end{aligned} \right\} \quad (3.1)$$

Note that the characteristic length of the trajectories of the particles, $\tilde{l} = \tilde{\Gamma}/(\tilde{V}_T \tilde{U}^{a-1})^{1/a}$, is of the order of $\tilde{\Gamma}/\tilde{V}_T$ for $a \simeq 1$. If $\beta \sim 1$ and V_T is small, the saddle point is also far from the vortex core in regions where the fluid acceleration is negligible and the characteristic scales are the same.

Substituting (3.1) in (2.2) we obtain a rescaled governing equation for the particles

$$\frac{\mathrm{d}^2 \hat{\boldsymbol{X}}}{\mathrm{d}\hat{t}^2} = \frac{\mathrm{d}\hat{\boldsymbol{V}}}{\mathrm{d}\hat{t}} = \frac{\beta - 1}{\beta + C_M} \frac{1}{F_p} (\hat{\boldsymbol{u}} - \hat{\boldsymbol{V}} - \boldsymbol{j}) + \frac{1 + C_M}{\beta + C_M} \frac{\mathrm{D}\hat{\boldsymbol{u}}}{\mathrm{D}\hat{t}}, \quad (3.2)$$

where $\boldsymbol{j} = -\boldsymbol{g}/|\boldsymbol{g}|$. The parameter F_p is a measure of the ratio of the particle inertia to the buoyancy forces and is defined by

$$F_p = V_T^{(1+1/a)} St = \left(\frac{\tilde{V}_T}{\tilde{U}} \right)^{1/a} \frac{\tilde{V}_T^2 \tilde{U}}{|\tilde{\boldsymbol{g}}|\tilde{\Gamma}} = \frac{\tilde{t}_p}{\tilde{\Gamma}/(\tilde{V}_T^{a+1} \tilde{U}^{a-1})^{1/a}}. \quad (3.3)$$

In physical terms, it can be expressed as a ratio of two characteristic lengths: the first being the distance over which a particle accelerates from zero velocity to the terminal velocity, $\tilde{V}_T \tilde{t}_p$, and the second being the minimum radius of curvature of trajectories of particles moving around line vortices, $\tilde{\Gamma}/\tilde{V}_T$. Note that when $a \simeq 1$, F_p is only dependent on $\tilde{\Gamma}$ and therefore does not depend on the radius of the vortex.

The rescaling of the inertial forces for the particles implies that the condition (2.3) of small particle diameter with respect to the characteristic size of the flow seen by

the particles (of the order of $\tilde{\Gamma}/\tilde{V}_T$) can be more precisely stated as

$$\frac{\tilde{d}_p \tilde{V}_T}{\tilde{\Gamma}} = \frac{(\beta-1)\tilde{d}_p^3 \tilde{g}}{18 k_T \tilde{v}^2 Re_f} \ll 1. \tag{3.4}$$

For the movement of particles around the smallest vortices of a turbulent flow, where $Re_f = \tilde{\Gamma}/\tilde{v} \sim 1$, this means that for particles in air, where β is of the order of 10^3, $\tilde{d}_p$ should be smaller than $10\,\mu\text{m}$. For this range of sizes, the parameter F_p can be large or small compared with unity. However, in water, most particles have comparable density, so that $\beta - 1 \sim 1$. In this case, $\tilde{d}_p$ should be smaller than $0.1\,\text{mm}$ in order for (3.4) to be valid. The equivalent condition for the local Reynolds number of the particles based on the relative velocity, $Re_T = \tilde{d}_p \tilde{V}_T/\tilde{v}$, is $Re_T \ll Re_f$. See Appendix A. This is also equivalent to $F_p \ll (\beta-1)/18 k_T Re_f$. Therefore, this model implies that for particles in turbulent flows of liquids where $V_T \sim 1$ or $V_T < 1$, F_p must be much less than one.

Provided $|\hat{\boldsymbol{u}} - \boldsymbol{j}|$ is $O(1)$, which means excluding regions near equilibrium points (defined by (2.7)), for small F_p the particle velocity normalized on V_T can be expanded as a series in F_p

$$\hat{\boldsymbol{V}} = \hat{\boldsymbol{u}} - \boldsymbol{j} - F_p \hat{\boldsymbol{V}}_{(1)} + F_p^2 \hat{\boldsymbol{V}}_{(2)} + \cdots, \tag{3.5}$$

where

$$\hat{\boldsymbol{V}}_{(1)} = \frac{\partial \hat{\boldsymbol{u}}}{\partial \hat{t}} + \left(\hat{\boldsymbol{u}} - \frac{\beta + C_M}{\beta - 1}\boldsymbol{j}\right) \cdot \nabla \hat{\boldsymbol{u}},$$

$$\hat{\boldsymbol{V}}_{(2)} = \frac{\beta + C_M}{\beta - 1}\left[\frac{\partial \hat{\boldsymbol{V}}_{(1)}}{\partial \hat{t}} + \hat{\boldsymbol{V}}_{(1)} \cdot \nabla \hat{\boldsymbol{u}} + (\hat{\boldsymbol{u}} - \boldsymbol{j}) \cdot \nabla \hat{\boldsymbol{V}}_{(1)}\right], \cdots$$

Hence,

$$\hat{\boldsymbol{V}} = \hat{\boldsymbol{u}} - \boldsymbol{j} - F_p \left[\frac{\partial \hat{\boldsymbol{u}}}{\partial \hat{t}} + \left(\hat{\boldsymbol{u}} - \frac{\beta + C_M}{\beta - 1}\boldsymbol{j}\right) \cdot \nabla \hat{\boldsymbol{u}}\right] + O(F_p^2). \tag{3.6}$$

This means that except within a distance $|\hat{\boldsymbol{X}} - \hat{\boldsymbol{X}}_E|$ of order F_p from the equilibrium points, the effect of a small inertia is of the order of F_p. Note that $\partial \hat{u}/\partial t = 0$ for a Rankine vortex.

The expansion (3.5) can be used to explain why particles tend to accumulate as a result of inertial forces. The velocity of the particles can be considered as a single-valued field if $F_p \ll 1$ (see (3.6)), assuming the particle concentration to be continuous. Thus, by taking the divergence of the particle velocity field, if the flow is incompressible

$$\nabla \cdot \boldsymbol{V} = -F_p \left[\frac{1}{4}\left(\frac{\partial u_i}{\partial x_j} + \frac{\partial u_j}{\partial x_i}\right)^2 - \frac{1}{4}\left(\frac{\partial u_i}{\partial x_j} - \frac{\partial u_j}{\partial x_i}\right)^2\right] + O(F_p^2), \tag{3.7}$$

which shows how inertial effects lead to divergence of particles from vortical regions and that particles tend to accumulate in regions of high strain rate and low vorticity. (See also Squires & Eaton 1991.) If $V_T < 1$, F_p is smaller than the Stokes number and therefore the rate of accumulation may be smaller than the value predicted by Maxey (1987) (his equation (5.10)), whose asymptotic analysis for small particle inertia was not focused on vortex flows.

Some further remarks on (3.6) should be made. The scaling (3.1) and the equation (3.6) are based on the assumption that the particles are moving in the outer region around the vortices and that $|\hat{\boldsymbol{u}} - \boldsymbol{j}|$ is $O(1)$. This may not occur if the particles

are released near the vortex cores. Also note that although the parameter V_T does not appear explicitly in (3.2) and (3.6), it has an implicit significance because $\hat{\boldsymbol{u}}$ is normalized on V_T. Expanding the expression of $\hat{\boldsymbol{u}}$ in terms of V_T, where (for the Rankine vortex)

$$\hat{\boldsymbol{u}} = \frac{-2\hat{y}}{V_T^2 + \hat{x}^2 + \hat{y}^2}\boldsymbol{i} + \frac{2\hat{x}}{V_T^2 + \hat{x}^2 + \hat{y}^2}\boldsymbol{j},$$

shows that this dependence is of the order of V_T^2 and therefore quite weak when $V_T \ll 1$.

3.2. *Asymptotic analysis for particles with small inertia far from singular regions*

Provided $|\hat{\boldsymbol{u}} - \boldsymbol{j}|$ is $O(1)$, it follows from (3.6) that the expansion (3.5) is valid for the whole domain if F_p is small. If F_p is of the order unity, the approximation is valid in a limited part of the domain where the acceleration in the velocity is small. If the acceleration is of $O(\mu F_p)$, μF_p would replace F_p in (3.5). This is the appropriate method for calculating the trajectories of particles when they are sufficiently far from the origin (see also Lasheras & Tio 1994). Then, the vortex appears as a point vortex with circulation $\tilde{\Gamma}$ whose azimuthal velocity $\tilde{u}_\theta$ varies as $\tilde{\Gamma}/|\tilde{\boldsymbol{x}}|$. By integrating $\mathrm{d}\hat{\boldsymbol{X}}/\mathrm{d}\hat{t} = \hat{\boldsymbol{V}}$ and using (3.5), the trajectory of a particle can also be expressed as an asymptotic series. If the coordinates of a particle released at time $\hat{t}_0$ from $(\hat{X}_0, \hat{Y}_0)$ are $\hat{\boldsymbol{X}} = (\hat{X}, \hat{Y})$ at time $\hat{t}_0 + \Delta\hat{t}$, such that $|\hat{\boldsymbol{X}}| \gg 1$, i.e. the particle moves far from the centreline of a vortex, they can be expanded as:

$$\left.\begin{array}{l} \varepsilon\hat{X} = \hat{X}_{(0)} + \varepsilon\hat{X}_{(1)} + \varepsilon^2\hat{X}_{(2)} + \cdots \\ \varepsilon\hat{Y} = \hat{Y}_{(0)} + \varepsilon\hat{Y}_{(1)} + \varepsilon^2\hat{Y}_{(2)} + \cdots \end{array}\right\} \tag{3.8}$$

where $\varepsilon = 1/|\hat{X}_0| \ll 1$. From (3.6) (with $\hat{u}_\theta = 2/|\hat{X}|$ for consistency with (2.5)), we obtain

$$\frac{\mathrm{d}\hat{X}_{(0)}}{\mathrm{d}\hat{t}} = 0, \quad \frac{\mathrm{d}\hat{Y}_{(0)}}{\mathrm{d}\hat{t}} = -\varepsilon,$$

$$\frac{\mathrm{d}\hat{X}_{(1)}}{\mathrm{d}\hat{t}} = \frac{-2\varepsilon\hat{Y}_{(0)}}{\hat{X}_{(0)}^2 + \hat{Y}_{(0)}^2}, \quad \frac{\mathrm{d}\hat{Y}_{(1)}}{\mathrm{d}\hat{t}} = \frac{2\varepsilon\hat{X}_{(0)}}{\hat{X}_{(0)}^2 + \hat{Y}_{(0)}^2},$$

$$\frac{\mathrm{d}\hat{X}_{(2)}}{\mathrm{d}\hat{t}} = \frac{-2(\hat{Y}_{(0)} + \varepsilon\hat{Y}_{(1)})}{(\hat{X}_{(0)} + \varepsilon\hat{X}_{(1)})^2 + (\hat{Y}_{(0)} + \varepsilon\hat{Y}_{(1)})^2} + \frac{2\hat{Y}_{(0)}}{\hat{X}_{(0)}^2 + \hat{Y}_{(0)}^2} + 2\varepsilon F_p\frac{\hat{Y}_{(0)}^2 - \hat{X}_{(0)}^2}{\hat{X}_{(0)}^2 + \hat{Y}_{(0)}^2},$$

$$\frac{\mathrm{d}\hat{Y}_{(2)}}{\mathrm{d}\hat{t}} = \frac{2(\hat{X}_{(0)} + \varepsilon\hat{X}_{(1)})}{(\hat{X}_{(0)} + \varepsilon\hat{X}_{(1)})^2 + (\hat{Y}_{(0)} + \varepsilon\hat{Y}_{(1)})^2} - \frac{2\hat{X}_{(0)}}{\hat{X}_{(0)}^2 + \hat{Y}_{(0)}^2} - 4\varepsilon F_p\frac{\hat{X}_{(0)}\hat{Y}_{(0)}}{\hat{X}_{(0)}^2 + \hat{Y}_{(0)}^2}.$$

Hence,

$$\hat{X} = \hat{X}_0 + \ln\frac{\hat{X}_0^2 + (\hat{Y}_0 - \Delta\hat{t})^2}{\hat{X}_0^2 + \hat{Y}_0^2} + O(\varepsilon, \varepsilon^2 V_T^2, \varepsilon F_p), \tag{3.9}$$

$$\hat{Y} = \hat{Y}_0 - \Delta\hat{t} + \hat{\theta}_1 + 2F_p\left[\frac{\hat{X}_0}{\hat{X}_0^2 + \hat{Y}_0^2} - \frac{\hat{X}_0}{\hat{X}_0^2 + (\hat{Y}_0 - \Delta\hat{t})^2}\right]$$

$$-\frac{2(\hat{Y}_0 - \Delta\hat{t})}{\hat{X}_0^2 + (\hat{Y}_0 - \Delta\hat{t})^2}\left[\ln\frac{\hat{X}_0^2 + (\hat{Y}_0 - \Delta\hat{t})^2}{\hat{X}_0^2 + \hat{Y}_0^2} + \frac{\hat{\theta}_1(\hat{Y}_0 - \Delta\hat{t})}{\hat{X}_0}\right] + O(\varepsilon^2, \varepsilon^2 V_T^2, \varepsilon^2 F_p^2),$$
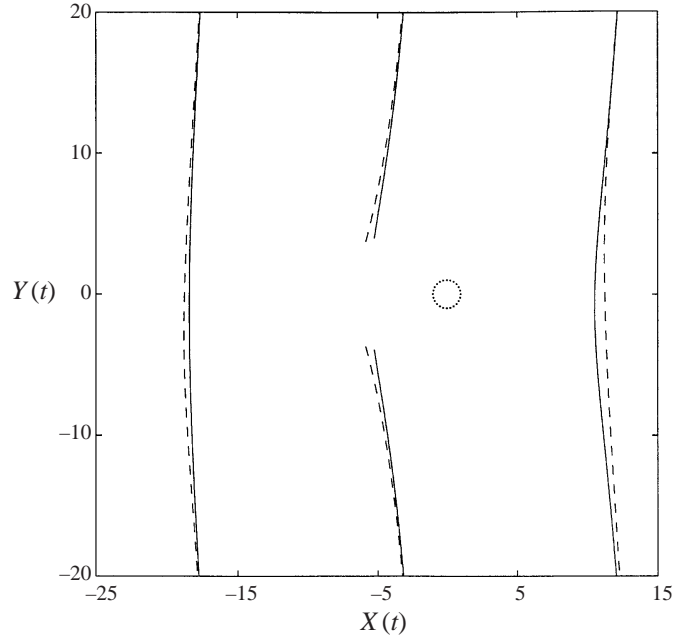
$$\tag{3.10}$$

FIGURE 3. Trajectories of particles for $F_p = 1$ and $V_T = 1$. ——, solution of the original system of (2.2). – – –, asymptotic expansion (3.9)–(3.10). Also a dotted circle with radius $1/V_T$ is shown as reference.

where

$$\tfrac{1}{2}\hat{\theta}_1 = \arctan\left(\frac{\hat{Y}_0}{\hat{X}_0}\right) - \arctan\left(\frac{\hat{Y}_0 - \Delta\hat{t}}{\hat{X}_0}\right).$$

Note that the extra displacement of particles induced by the vortex $\Delta\xi = \hat{X} - \hat{X}_0$, increases without limit, but $\Delta\eta = \Delta\hat{Y} + \Delta\hat{t} = \hat{Y} - (\hat{Y}_0 - \Delta\hat{t})$ reaches a finite limit as $\Delta\hat{t} \to \infty$. Their dependence on the inertia and on the terminal velocity is of order εF_p or $\varepsilon^2 V_T^2$ for $|X| \gg 1$ and therefore tends to zero as $|\hat{X}| \to \infty$. In figure 3, we have plotted some trajectories of particles for $F_p = 1$ and $V_T = 1$. Comparing the numerical solution of the original system (2.2) (solid line) with the trajectories obtained from the asymptotic analysis in (3.9) and (3.10) (dashed line) shows close agreement far from the origin of the vortex. These asymptotic results are also quantitatively applicable to the irrotational regions of all types of flow far from any confined region of vorticity.

4. Singular features of particle settling near line vortices

Note that the dynamical system (2.2) has dimension 4 (i.e. X, V). However, when $F_p \ll 1$, the system becomes two-dimensional and V can be expressed as a function of X, as shown by (3.6), independently of the initial position or velocity of the particle. If the particle's inertia is small, they match the surrounding flow and gravity conditions ($\Delta V \sim V_T + u - V$) in a short time interval $\Delta t \sim St$, i.e. $\Delta\hat{t} \sim F_p$ (see (3.6)). However, if the inertia of the particles is finite, the history of the particles' motion is significant. When falling from above, the vortices do not reach the equilibrium points with zero velocity. In this case, there may still be a particle stagnation point X_P where $V = 0$,

but, in general, $\mathrm{d}\boldsymbol{V}/\mathrm{d}t \neq 0$ at $\boldsymbol{X} = \boldsymbol{X}_P$. $\boldsymbol{X}_P$ is on the same side of the vortex as $\boldsymbol{X}_{E2}$ and for $F_p \ll 1$, $|\boldsymbol{X}_P - \boldsymbol{X}_{E2}| \ll 1$.

In most practical situations, the particles are released above the vortices. For particles with small inertia some 'empty' regions may appear (Raju & Meiburg 1995). The geometry of these empty regions strongly depends on the terminal velocity. In figure 4(*a*) the limit trajectories of (2.2) (with initial condition $V = 0$ at $\boldsymbol{X}_{E2}$) are shown for different values of V_T for $St = 0.125$ and $\beta \to \infty$. As we have already mentioned, the radial distance of the equilibrium point $\boldsymbol{X}_{E2}$ increases in proportion to $1/V_T$. As a consequence, the region enclosed between the limit trajectories becomes wider as V_T decreases. The dependence on the Stokes number is shown in figure 4(*b*), where we have plotted the limit trajectories for $\beta \to \infty$, $V_T = 0.2$ and $St = 0.5$, 2 and 8.

Figure 4(*b*) shows how the region enclosed by the two limit trajectories varies in size and form as the particle inertia (F_p) increases, which implies that the empty region for particles with small inertia also changes with F_p. However, when F_p is large, the particles can cross the limit trajectories and the empty region may disappear. These effects are shown quantitatively in figure 5 through a plot of the non-dimensional asymptotic width $\hat{W}_e$ (as $\hat{y} \to -\infty$) of the strip of the empty region created by a Rankine vortex as a function of F_p and of the normalized terminal velocity V_T. For small values of F_p, $\hat{W}_e$ is of the order of the product of F_p and the time it takes to go around the vortex (see (3.6)). Therefore,

$$\hat{W}_e \propto F_p, \tag{4.1}$$

in agreement with our calculations. Since $\hat{V} = 0$ at $\boldsymbol{X}_{E2}$, the proportionality constant has a large value, e.g. $\hat{W}_e \sim 40 F_p$ for $V_T = 0.1$.

For larger values of F_p, the increased inertia of the particles prevents them from responding to the vortex flow, to such an extent that some of them even cross the limit trajectories. Then, naturally, $\hat{W}_e$ decreases (see figure 6). These arguments are consistent with the computations which show that $\hat{W}_e$ increases with F_p until $F_p \sim 1$, above which $\hat{W}_e$ rapidly decreases. The maximum value of $\hat{W}_e$ is related to the nonlinear processes appearing around the saddle point $\boldsymbol{X}_{E2}$. For $V_T \sim 1$, it depends strongly on the local values of the velocity in the vortex core.

Empty regions and equilibrium points vanish when the value of V_T increases sufficiently that, even if F_p is small, the particles cut through the vortex. However, in many aerosol-particle motions with significant fluid acceleration, i.e. $F_f \gg 1$, the particle Froude number $F_p \sim 1$ and the fall speed is small, i.e. $V_T < 1$. In this case, open empty regions appear and the width of the strip is largely related to the effect of particle inertia, effectively the value of $F_p = St^3/F_f^2$ (table 1). In figure 5, we have also plotted the thickness of the empty region for constant values of the flow Froude number (dashed lines), indicating the situations appearing in a certain flow with particles of different properties. Note that for values of $V_T > 1$, there are no equilibrium points and $\hat{W}_e \to 0$. Similar effects can be expected in other flows with concentrated vorticity, where saddle points create regions which cannot be reached by particles with finite inertia.

For a better understanding of the effect of the particle inertia, we now analyse the trajectories of aerosol particles near the equilibrium points $\boldsymbol{X}_{E2}$. Note how, in figure 6, a trajectory passing close to the equilibrium point $\boldsymbol{X}_{E2}$ has an abrupt change in its direction and then crosses other trajectories. Sudden changes in the direction of the velocity of particles were noted by Maxey & Corrsin (1986; see their figure 9). In
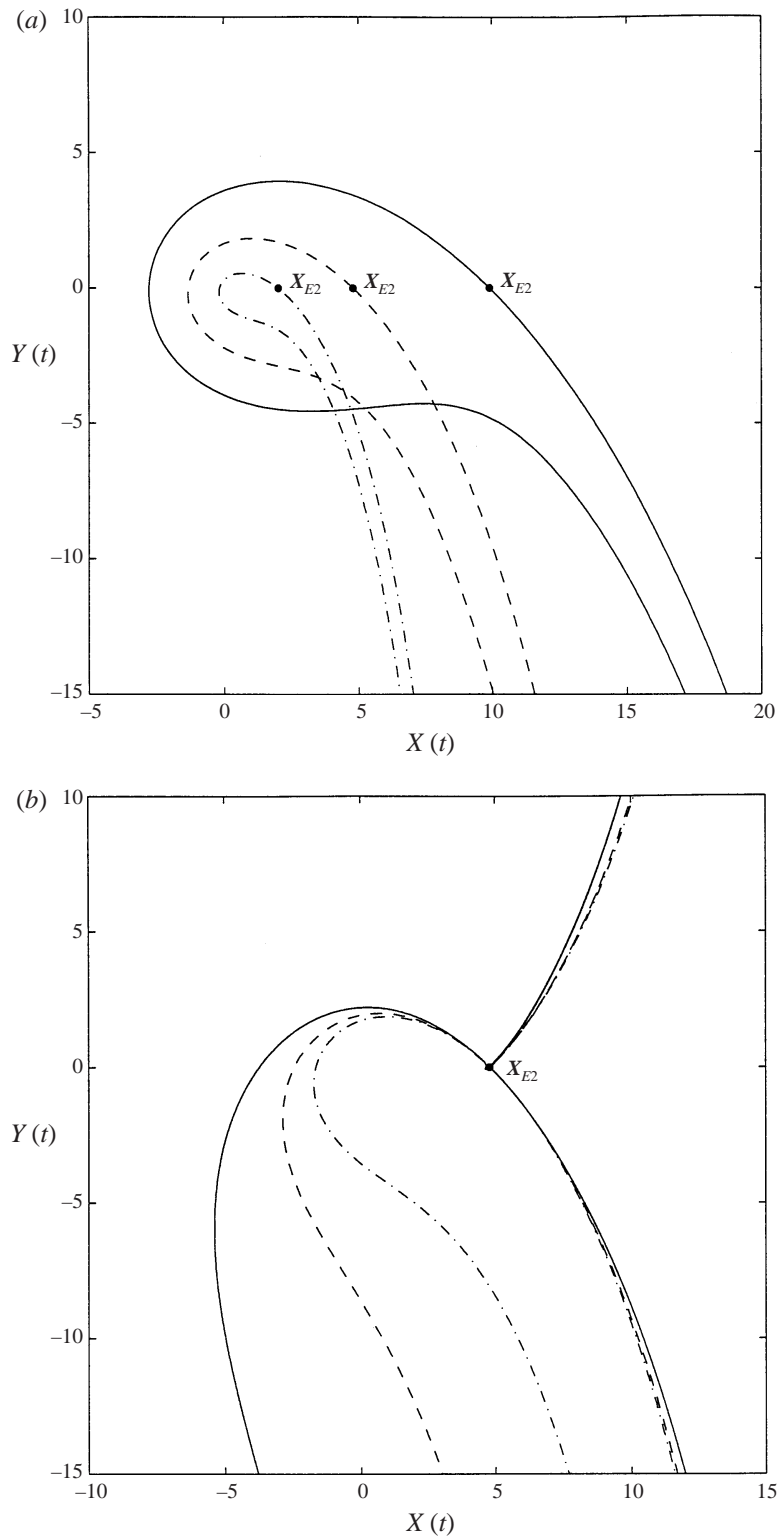
FIGURE 4. (a) Limit trajectories of inertial particles for fixed $St = 0.125$. ———, $V_T = 0.2$ ($F_p = 0.005$); ———, $V_T = 0.4$ ($F_p = 0.02$); — · —, $V_T = 0.8$ ($F_p = 0.08$). (b) Limit trajectories of inertial particles having the same $V_T = 0.4$ (and saddle point X_{E2}). — · —, $St = 0.5$ ($F_p = 0.08$); ———, $St = 2$ ($F_p = 0.32$); ———, $St = 8$ ($F_p = 1.28$).
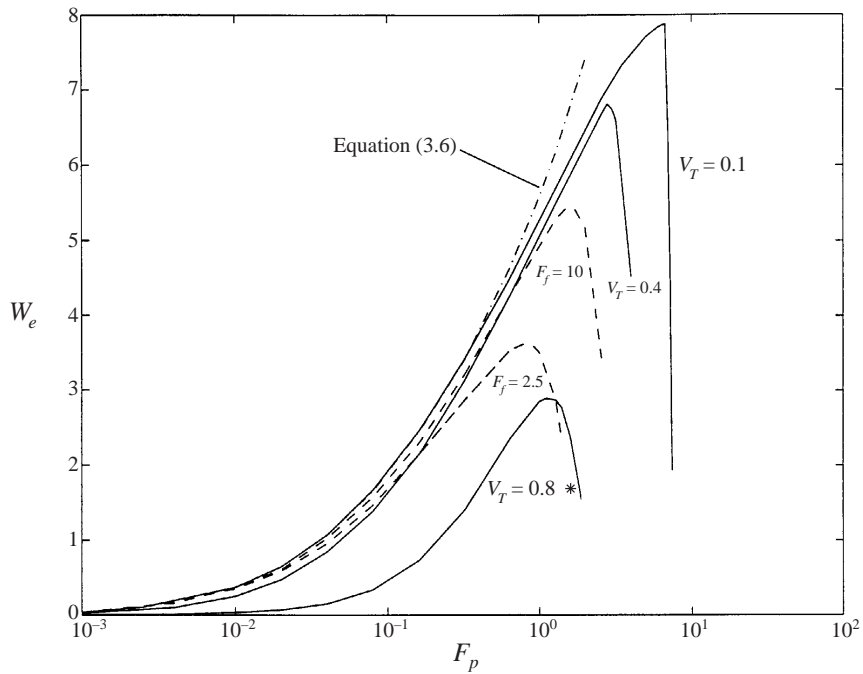
FIGURE 5. Asymptotic dimensionless width $\hat{W}_e$ of the empty region for $V_T = 0.1$, 0.4 and 0.8 as the inertial Froude number of the particles F_p increases over the range 10^{-3} to 10. ——, $\hat{W}_e$ versus F_p for constant value of V_T; $- \cdot -$, $\hat{W}_e$ versus F_p for $V_T = 0.1$ calculated using (3.6); $---$, $\hat{W}_e$ versus F_p for constant values of the flow Froude number F_f.
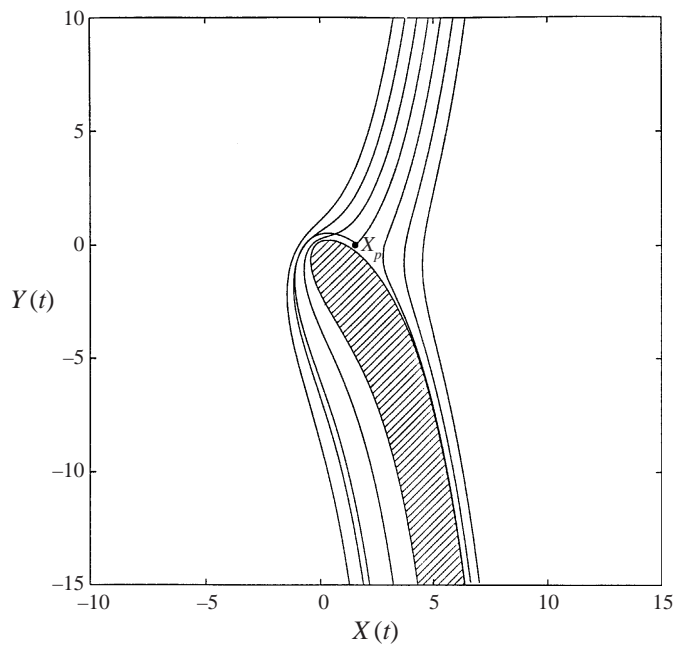
FIGURE 6. Trajectories $(\hat{X}(t), \hat{Y}(t))$ of inertial particles where $V_T = 0.8$ and $F_p = 1.8$ (marked by an asterisk in figure 5). Notice that the central trajectory crosses some of the outer ones. The shadowed region represents the positions that the particles cannot reach ('empty region').
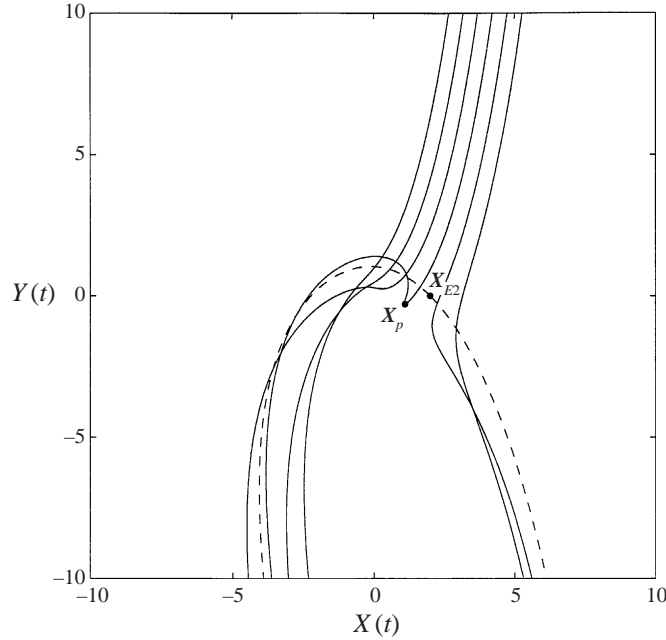
FIGURE 7. —, trajectories of inertial particles near the particle stagnation point X_P for $F_p = 4$ and $V_T = 0.1$; $---$, limit trajectories.

regions where $\boldsymbol{u} - \boldsymbol{V}_T \sim St$ (or $\hat{\boldsymbol{u}} - \boldsymbol{j} \sim F_p$), the effect of the particle inertia changes the trajectory even if F_p is very small (see (3.2)). Consider a particle approaching X_{E2}; it cannot react instantaneously to the flow conditions and, as a consequence, it may cross one of the limit trajectories. Once the particle has crossed the limit trajectory, the local direction of the combined vector $\boldsymbol{u} + \boldsymbol{V}_T$ is opposite to that of the velocity of the particle at that point. From (2.6), it follows that the small changes in the particle velocity can occur over a time δt and a distance δX where

$$\delta t = \frac{\delta X}{V} = St \frac{\delta V}{\boldsymbol{u} + \boldsymbol{V}_T - \boldsymbol{V}}. \tag{4.2}$$

For the particle velocity to come to rest from its initial velocity, $|\delta V| \sim V_T$. This takes a distance $|\delta X| \sim V_T St$ or smaller. Since for a line vortex $|X_{E2}| \sim 1/V_T$, this implies that $|\delta X|/|X_{E2}| \sim V_T^2 St = F_p$. Therefore, if F_p is of order unity or less, the particle reaches a velocity zero at a particle stagnation point (PSP) X_P near the equilibrium point X_{E2}. The larger F_p is, the greater is the distance between the equilibrium point X_{E2} (where $\boldsymbol{u} + \boldsymbol{V}_T = 0$ and $V = \dot{V} = 0$) and the PSP X_P, and the position of X_P moves closer to the vortex. Note that at the PSP, $\boldsymbol{u} + \boldsymbol{V}_T \neq 0$ and there is locally a large acceleration given by $d\boldsymbol{V}/dt = (1/St)(\boldsymbol{u} + \boldsymbol{V}_T)$ which has the opposite sign to $\boldsymbol{V}_T$ and $\boldsymbol{V}$. Figure 7 shows how this results in a sharp corner in the trajectory of the particle at X_P. When F_p increases above a certain value F_{p_m}, V is never zero anywhere and no PSP exists. The characteristic stopping distance for a particle with small inertia is $|\hat{X}_{E2} - \hat{X}_{E1}| = |X_{E2} - X_{E1}|V_T = 2\sqrt{1 - V_T^2}$ (for $V_T < 1$). Thus, the overshooting effect is greater for smaller values of V_T, in agreement with our numerical finding that the critical value F_{p_m}, for which there are no more turning points, increases whenever V_T decreases. In figure 7, we have plotted the trajectories of particles for $F_p = 4$ and $V_T = 0.1$ near the saddle point X_{E2}. The actual particle

stagnation point X_P is marked. Since the value of the inertia parameter is relatively large and V_T is small, it is evident that the direction of the velocity of the particles changes over a large scale of the order of F_p. This phenomenon has also been studied on the saddle points of a two-dimensional shear layer by Martin & Meiburg (1994).

Up to this point, we have consolidated some ideas about the basic features of particles moving around vortices. In the following section, we define global quantitative expressions for the concepts established in §§ 3 and 4.

5. Settling of particles near a Rankine vortex

The sedimentation of particles in complex flows is best understood in terms of the horizontal and vertical displacement differences $(\Delta\xi, \Delta\eta)$ between the displacements $\Delta\hat{X}, \Delta\hat{Y}$ of particles moving in the flow and those $\Delta\hat{X}_T, \Delta\hat{Y}_T$ in the still fluid over the same time interval $\Delta\hat{t} = \Delta\tilde{T}_T(\tilde{V}_T^2/\tilde{\Gamma})$. The dimensionless displacements, for particles released at $\hat{X}_0, \hat{Y}_0$ at $\hat{t} = 0$, can be defined as

$$\Delta\hat{X}(\hat{X}_0, \hat{X}, \Delta\hat{t}) = \hat{X}(\hat{X}_0, \Delta\hat{t}) - \hat{X}_0,$$
$$\Delta\hat{Y}(\hat{X}_0, \hat{X}, \Delta\hat{t}) = \hat{Y}(\hat{X}_0, \Delta\hat{t}) - \hat{Y}_0. \tag{5.1a}$$

These can be expressed in terms of perturbations from their values in still fluid $\Delta\hat{X}_T = 0$ and $\Delta\hat{Y}_T = -\Delta\hat{t}$,

$$\left.\begin{array}{l} \Delta\xi = \Delta\hat{X} - \Delta\hat{X}_T = \Delta\hat{X}, \\ \Delta\eta = \Delta\hat{Y} - \Delta\hat{Y}_T = \Delta\hat{Y} + \Delta\hat{t}. \end{array}\right\} \tag{5.1b}$$

If the particle settling is slowed down by the vortex, $|\Delta\hat{Y}|$ is less than in still fluid, i.e. $\Delta\eta > 0$. To analyse the overall effect of the vortex, we consider trajectories between two levels $\hat{Y} = \pm\hat{Y}_0$ well above or below the vortex, i.e. $\hat{Y}_0 \gg 1$ and $\Delta\hat{t} = 2\hat{Y}_0$ (see (3.9)–(3.10)). Under these conditions, $\Delta\xi$ and $\Delta\eta$ are only functions of $\hat{X}_0$ and of the dimensionless parameters of the problem, F_p and V_T. In figures 8(a)– 8(c) we have plotted $\Delta\eta$ versus $\hat{X}_0$ for $\Delta\hat{t} = 2 \times 10^4$, $\hat{Y}_0 = 10^4$, $F_p = 1$, and $V_T = 0.4, 1.2$ and 5. A strong peak appears when the dimensionless terminal velocity V_T is smaller than one and the stopping distance of the particles is of the order of the radius of the vortex or smaller (i.e. $F_p < O(1)$) (figure 8a). Owing to the existence of the turning points X_P, the particles spend a long time near these points. Particles having initial positions $(\hat{X}_0, \hat{Y}_0)$ far from the vortex with $|\hat{X}_0| \gg 1$, whatever the values of F_p and V_T, almost follow straight lines and $\Delta\eta \ll 1$. When $\tilde{V}_T$ is greater than the maximum vertical velocity of the vortex (i.e. $V_T > 1$), there can be no equilibrium points and the peak in $\Delta\eta$ becomes finite, as shown in figure 8(b). Finally, if the particles have a large V_T, they move with velocities close to the terminal velocity and $\Delta\eta$ is small for any value of $\hat{X}_0$ (figure 8c).

In figure 9, we have plotted the maximum value of $\Delta\eta$ versus F_p for $V_T = 0.1$, 0.4, 0.7 and 1.0 . Decreasing F_p for a given value of V_T, we reach a critical value $F_{p_m}(V_T)$ (independent of $\hat{Y}_0$) below which the maximum value of $\Delta\eta$ increases very rapidly. In order to understand this behaviour, we have calculated many trajectories of particles for values of F_p close to F_{p_m} and for different V_T. As we would expect, F_{p_m} corresponds to the limit value of F_p above which there is no particle stagnation point. As shown in §4, this phenomenon of overshooting only appears for small and intermediate values of F_p and is more marked for smaller values of V_T. This is consistent with the dependence of F_{p_m} on V_T, which, as figure 9 shows, decreases
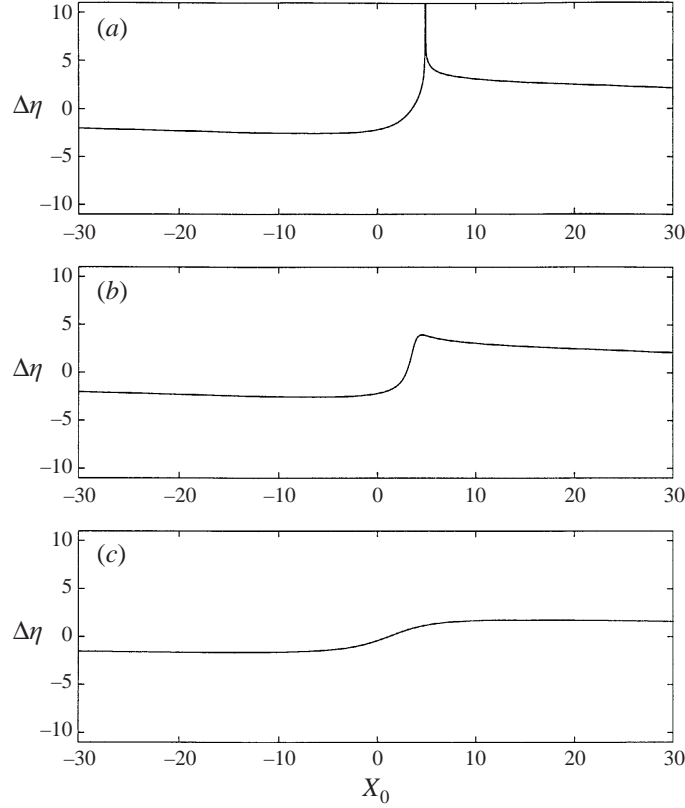
FIGURE 8. Dimensionless differential settling length $\Delta\eta$ (normalized on a length $\tilde{\Gamma}/\tilde{V}_T$) versus the initial horizontal position of the inertial particles, $\hat{X}_0$ for $\hat{Y}_0 = 10^4$, $\Delta\hat{t} = 2 \times 10^4$, and $F_p = 1$. (a) $V_T = 0.4$, (b) $V_T = 1.2$, (c) $V_T = 5$.

when V_T increases. We show below that F_{p_m} is also a critical value for the dependence of the bulk settling velocity on F_p.

Since the initial position of particles moving in a complex flow is random, we must define a mean settling length $\langle \Delta\hat{Y} \rangle$ averaged over all initial positions in relation to a fixed time, say $\Delta\hat{t}$, in terms of the average displacement difference $\langle \Delta\eta \rangle$ as

$$\langle \Delta\hat{Y} \rangle = \frac{1}{\hat{L}_x} \int_{-\hat{L}_x/2}^{\hat{L}_x/2} \Delta\hat{Y} \, d\hat{x}_0 = \langle \Delta\eta \rangle - \Delta\hat{t}, \tag{5.2}$$

where $\hat{L}_x$ is the dimensionless distance over which the average is made and $\Delta\hat{Y}$ is defined in (5.1a). In order to study the local effect of a single vortex, we express $\langle \Delta\eta \rangle$ as

$$\langle \Delta\eta \rangle = \frac{1}{\hat{L}_x} \left[D + f\left(\frac{\hat{Y}_0}{\hat{L}_x} \right) \right], \tag{5.3}$$

where D is a drift integral of $\Delta\eta$,

$$D = \int_{-\infty}^{\infty} \Delta\eta(\hat{X}_0) \, d\hat{X}_0, \tag{5.4}$$

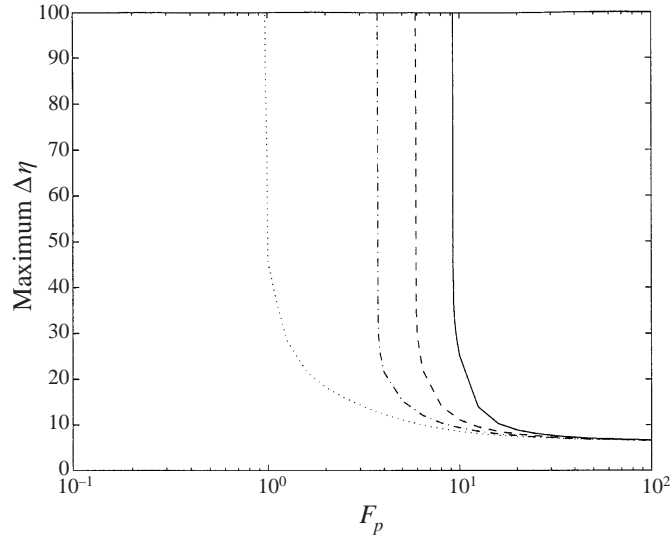which is independent of $\hat{Y}_0$ and is only a function of F_p and V_T if $\hat{Y}_0 \to \infty$. The

FIGURE 9. Maximum value of the normalized differential settling length $\Delta\eta$ versus the particle Froude number F_p for ———, $V_T = 0.1$; – – –, $V_T = 0.4$; – · –, $V_T = 0.7$; · · ·, $V_T = 1$. For any V_T, F_{p_m} corresponds to the value of F_p for which $\Delta\eta$ goes to infinity.

function $f(\hat{Y}_0/\hat{L}_x)$ depends on $\hat{Y}_0$, but does not depend on F_p and V_T (see § 3.2) and is defined (from (5.1a) and (5.2)) by

$$f(\hat{Y}_0/\hat{L}_x) = -\int_{\hat{L}_x/2}^{\infty} [\Delta\hat{Y}(\hat{X}_0) + \Delta\hat{Y}(-\hat{X}_0) + 2\Delta\hat{t}]\,\mathrm{d}\hat{X}_0, \qquad (5.5)$$

where it is assumed that $\hat{L}_x \gg 1$. From (3.10), we obtain (ignoring higher-order terms)

$$f\left(\frac{\hat{Y}_0}{\hat{L}_x}\right) = 16\int_0^{\arctan(2\hat{Y}_0/\hat{L}_x)} r\tan r\,\mathrm{d}r. \qquad (5.6)$$

To simplify the problem, we have assumed large horizontal averaging settling length $\hat{L}_x$ so that $\hat{Y}_0/\hat{L}_x \to 0$ and $f(\hat{Y}_0/\hat{L}_x) = 0$. Later, we show that the result of the bulk settling velocity does not depend on $\hat{Y}_0/\hat{L}_x$ if $\hat{Y}_0 \to \infty$.

The numerical integration of D has been carried out by two different procedures: the trapezoidal rule and a fourth-order Runge–Kutta. To reduce numerical errors, the asymptotic results presented in § 3.2 have been used. In figure 10, D is plotted versus F_p for different values of the dimensionless terminal velocity. The same asymptotic value was reached for $F_p \to 0$ as is obtained by integrating (3.6) instead of (2.2). The positive peaks in $\Delta\eta$, shown in figure 8, make only a small contribution to the drift integral, because the logarithm of $\Delta\hat{Y}$ close to the saddle point, when integrated, tends to a contribution of the order of $O[(\hat{X}_0 - \hat{X}_0^*)\log(\hat{X}_0 - \hat{X}_0^*)]$, which tends to zero as $(\hat{X}_0 - \hat{X}_0^*) \to 0$. There is a value F_p^* for which D is zero so that, for $F_p < F_p^*$, the drift integral $D < 0$, which means that particles fall faster in the presence of the vortex. In the inertialess limit of $F_p \to 0$, the negative drift integral D increases with V_T (figure 11), but suddenly decreases to zero when $V_T > 1$ because no equilibrium point exists and the 'empty' region disappears. For $F_p > 0$, the smaller V_T is, the greater is $|D|$, because the empty region becomes larger relative to $\tilde{\Gamma}/\tilde{V}_T$.

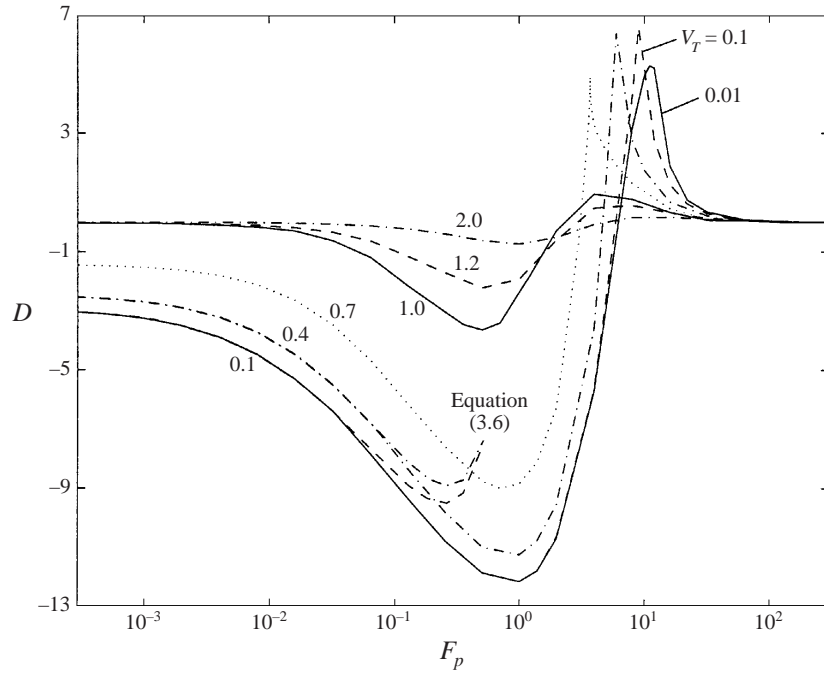When F_p increases up to a maximum value F_{p_M}, the drift becomes more negative as

FIGURE 10. Normalized 'drift' integral $D = \int \Delta \eta \, d\hat{X}$ versus F_p for $V_T = 0.01, 0.1, 0.4, 0.7, 1, 1.2, 2$. Notice that the peaks of the curves for $V_T = 0.1, 0.4$ and 0.7 correspond to the values $F_p = F_{p_m}$ of figure 9. The dashed line has been calculated using (3.6) to obtain the trajectories of the particles.
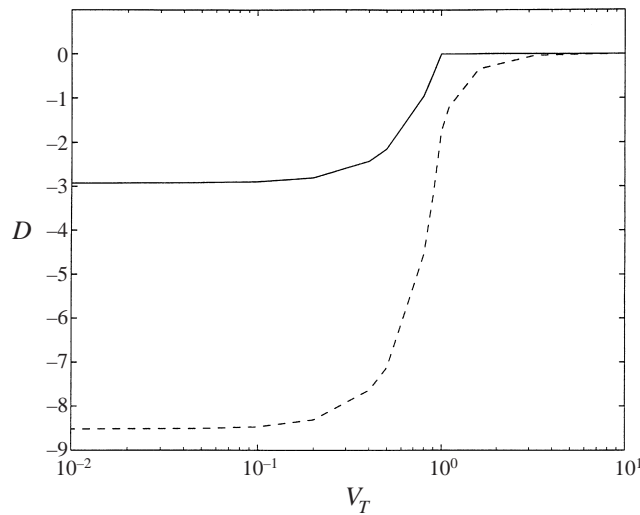

FIGURE 11. Normalized drift integral D of non-inertial particles versus V_T for ——, $F_p = 0$; ---, 0.1.

a consequence of the inertial effect shown by (3.7) for any value of V_T. The particles displaced towards the downflow side of the vortex (negative values of $\hat{X}$ in our case), as a result of the inertia, do not return to the upflow side and therefore fall faster. This tendency also increases the width of the empty region, $\hat{W}_e$. As figure 5 shows, this increases as F_p increases until the inertia of the particle and F_p are large enough that
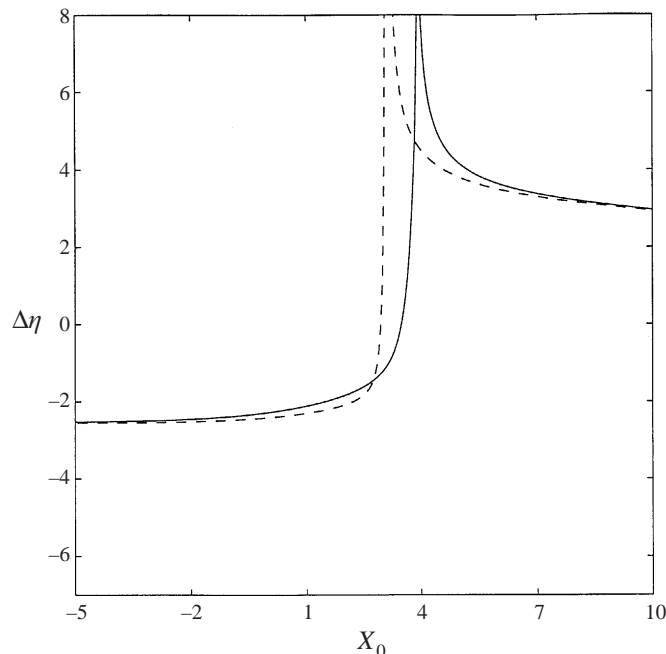
FIGURE 12. Dimensionless differential settling length $\Delta\eta$ versus the initial horizontal position of the particles $\hat{X}_0$ for $\hat{Y}_0 = 10^4$, $\Delta\hat{t} = 2 \times 10^4$, $V_T = 0.2$ and ——, $F_p = 4$; $---$, 8.

any deflection by the vortex is very small. Note that the increase in $\hat{W}_e$ is correlated with the increase of $(-D)$.

When $F_p \sim 1$, the particle inertia is so strong that some trajectories coming from above the vortex with a negative vertical velocity cross through the limit trajectories to the upflow side that pass through X_P, as shown in figures 6 and 7. Positive values of the drift integral D are found for $F_p > F_p^*$. To explain this fact, we have plotted $\Delta\eta$ versus $\hat{X}_0$ for $V_T = 0.2$ and $F_p = 4$ and 8 in figure 12. The peak in $\Delta\eta$, which corresponds to the trajectories passing near the PSP X_P broadens for larger values of F_p. This is related to the phenomenon of 'overshooting' discussed in §4. Owing to the delay in the particle response to the flow conditions, sudden changes in the velocity direction occur, which means that the particles effectively take a longer time to settle. This happens when trajectories cross the region where $|\hat{\boldsymbol{u}} - \boldsymbol{j}| \sim F_p$, so that there is a wider range of initial locations $\hat{X}_0$ where $\Delta\eta$ is large. Moreover, the peak moves towards lower values of $\hat{X}_0$ since particles with larger inertia describe straighter trajectories when they move above the vortex. The result of both tendencies is that the particles settle more slowly and there is an increase of the drift integral.

As shown in figure 9, when F_p exceeds F_{p_m} the particle stagnation points, where $V_y = 0$, disappear. Then, the peak of $\Delta\eta$ is finite and decreases monotonically as F_p increases. This is shown in figure 13 where we have plotted the settling length versus the initial position of the particles for $V_T = 0.4$ and $F_p = 7$, 8 and 9. Note that for these values, there is no significant change in the position of the peak. Since the drift integral D is largely determined by the 'area' under the peak when $F_p > 1$, the maximum value of D is reached for $F_p \simeq F_{p_m}$ and decreases monotonically as F_p increases. Large values of D can be found for smaller V_T because, as mentioned in §4, the region where sudden changes in the direction on the velocity of particles can
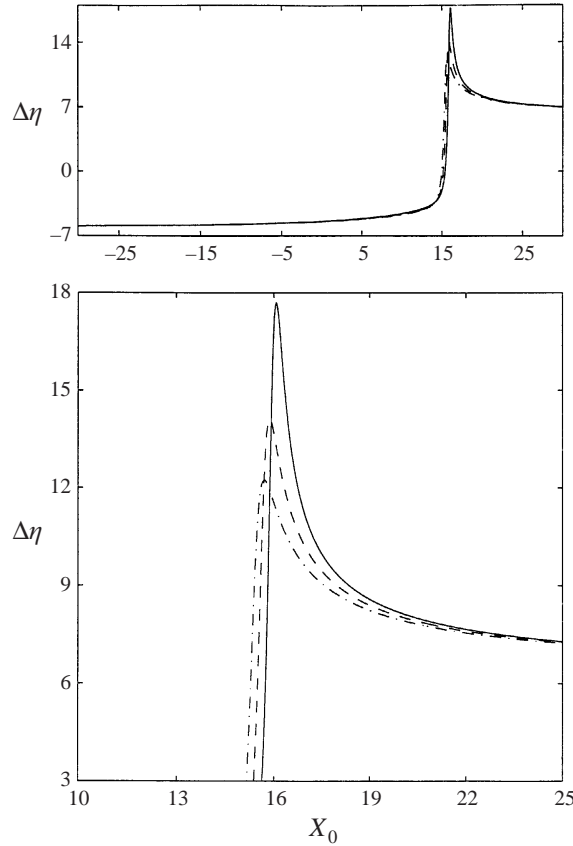
FIGURE 13. Dimensionless settling length $\Delta\eta$ versus the initial horizontal position of the particles $\hat{X}_0$ for $\hat{Y}_0 = 10^4$, $\Delta\hat{t} = 2 \times 10^4$, $V_T = 0.4$. ———, $F_p = 7$; – – –, $F_p = 8$; – · –, $F_p = 9$.

occur increases whenever V_T decreases. Thus, the value of D can be relatively large if there are vortices with F_p close to F_{p_m} for small values of V_T.

This shows again the importance of the particles' inertia and, in particular, the importance of the overshooting phenomenon in this problem. Clearly, the asymptotic approximations for small inertia parameters give misleading estimates of the settling process both qualitatively and quantitatively.

6. The bulk settling velocity in vortex flows

If the bulk settling velocity $\langle \tilde{V}_y \rangle_B$ is defined as the reciprocal of the mean time $\langle \Delta\tilde{T} \rangle$ for particles to fall between two levels a distance $\tilde{Y}_0 - \tilde{Y}_1$ apart (where $\tilde{Y}_0 > \tilde{Y}_1$), then $\langle \tilde{V}_y \rangle_B = (\tilde{Y}_0 - \tilde{Y}_1)/\langle \Delta\tilde{T} \rangle$. Here, the mean is taken over all initial positions at the level $\tilde{Y}_0$. Now, if the particles fall a large distance past the vortex, $\Delta\tilde{T}$ can be expressed as a function of the drift integral D (see (1.2) and (5.3)),

$$\langle \tilde{V}_y \rangle_B = \frac{\tilde{V}_T}{1 + D/(\hat{Y}_0 - \hat{Y}_1)\hat{L}_x}. \tag{6.1}$$

This is not equal to the average velocity along the trajectory, which is defined in (1.1) as

$$\langle \tilde{V}_y \rangle_L = \tilde{V}_T - \frac{\langle \Delta\tilde{\eta} \rangle}{(\tilde{Y}_0 - \tilde{Y}_1)} \tilde{V}_T = \tilde{V}_T \left[1 - \frac{D}{(\hat{Y}_0 - \hat{Y}_1)\hat{L}_x} \right]. \tag{6.2}$$

Equations (6.1) and (6.2) show that, since D is finite, the average bulk and Lagrangian settling velocity of particles near a single but infinite vortex between two planes very far apart is asymptotically equal to the terminal velocity $\tilde{V}_T$ in still fluid for any value of the inertia parameter and for any value of the terminal velocity. However, in the real flows of natural and industrial processes, the average settling velocity is effectively defined over finite regions around each vortex. Therefore, comparing (6.1) and (6.2), the bulk and Lagrangian settling velocities differ from each other and from the terminal velocity, because the characteristic length of the trajectories of the particles $\tilde{\Gamma}/\tilde{V}_T$ is not much less than the characteristic horizontal and vertical distances between vortices $\tilde{L}_x$ and $\tilde{Y}_0$.

Although there are no general methods for predicting the value of $\langle \tilde{V}_y \rangle_B$ in turbulence flows, our analysis indicates its general dependence on F_p and V_T if these parameters are suitably redefined in terms of the most energetic vortices in these flows. Consider a three-dimensional flow composed of N groups of distinct vortex tubes defined by a circulation $\tilde{\Gamma}_i$, a radius $\tilde{R}_i$, a length $\tilde{L}_i$, and a unitary vector parallel to the axis $\boldsymbol{n}_i$. The resulting bulk settling velocity, obtained by adding the effect of every vortex, is

$$\tilde{V}_B = \tilde{V}_T \left[1 - \sum_{i=1}^{N} \alpha_i D(F_{pi}, V_{Ti}) \right], \tag{6.3}$$

where α_i is the effective volume fraction within which the trajectories of the particles are distorted by the vortex, $(\tilde{\Gamma}_i/\tilde{V}_{Ti})^2 \tilde{L}_i$, divided by the volume occupied by a vortex of the i group, and $D(F_{pi}, V_{Ti})$ is the drift integral of the differential settling length. The local particle Froude number is

$$F_{pi} = \frac{\tilde{\tau}_p \tilde{\Gamma}_i}{\tilde{R}_i^2} V_{Ti}^2 = \frac{\tilde{\tau}_p^3}{\tilde{\Gamma}_i} [\tilde{\boldsymbol{g}} - (\tilde{\boldsymbol{g}} \cdot \boldsymbol{n}_i)\boldsymbol{n}_i]^2,$$

and the equivalent dimensionless terminal velocity for each vortex (removing the effect of gravity due to the component parallel to its axis) is

$$V_{Ti} = \frac{\tilde{\tau}_p \tilde{R}_i}{\tilde{\Gamma}_i} |\tilde{\boldsymbol{g}} - (\tilde{\boldsymbol{g}} \cdot \boldsymbol{n}_i)\boldsymbol{n}_i|.$$

The reason why this idealized model is relevant to the settling of particles in turbulence is because flow visualization (e.g. Perkins, Ghosh & Phillips 1991) and direct numerical simulations (e.g. Squires & Eaton 1991; Vincent & Meneguzzi 1994) have shown that in most three-dimensional turbulent flows, distinct elongated coherent vortices occur. Usually, they have a length that scales with the integral scale L_x and a radius that scales with the Kolmogorov microscale (Jiménez *et al.* 1993). Only those vortices with the largest circulation and whose axes are approximately horizontal have a large effect on particle settling. Based on these observations, our result in figure 10 suggests that for $0 < V_T < O(1)$ and $F_p < O(1)$, the average settling speeds rises to a maximum value of above 80% of the settling velocity in still fluid. How do these suggestions compare to previous investigations and to experiments?

The numerical simulations of heavy particles in isotropic homogeneous turbulence performed for Re_λ from 20 to 60 by Wang & Maxey (1993) showed a significant increase in the Lagrangian average vertical velocity $\langle \tilde{V}_y \rangle_L$ for particles with viscous response time and terminal velocity comparable to the Kolmogorov scales of the turbulence. In their simulations, the value of F_p associated with the smaller scales was of the order of unity. Hence, for the large-scale structures of the flow, F_p would

be very small, corresponding to regions where there is no concentration of particles
(see (3.7)). They found that the transient time for the concentration field and for
$\langle \tilde{V}_y \rangle_L$ averaged over many particles is of the order of the integral timescale of the
turbulence. This suggests that the particles need a time of that order of magnitude to
find themselves in the locality of significant vorticity (of scale η_K). Thus, the distance
between the vortices is much larger than their radii and we can apply our results. We
also have to assume that the local vortical structures are approximately steady for
time intervals of the order of magnitude of the settling of the particles. Vincent &
Meneguzzi (1994) found that the lifetime of these intense vortical structures is of the
order of the eddy turnover time, $\tilde{T}_E$. Hence, $\tilde{T}_E$ should be much larger than $\tilde{\Gamma}/\tilde{V}_T^2$
(see (3.1)). In this case, the bulk settling velocity would be

$$\langle \tilde{V}_y \rangle_B \simeq \langle \tilde{V}_y \rangle_L = \tilde{V}_T[1 - \bar{\alpha}\bar{D}], \tag{6.4}$$

where $\bar{\alpha}$ is the effective volume fraction occupied by the vortices and $\bar{D}$ is an average
value of the drift integral for the different values of F_p and V_T appearing in the flow.
Therefore, if these two dimensionless parameters are at most of the order of unity,
$\bar{D}$ would be always negative (see figure 10) with a minimum for $F_p = St V_T^2 \sim 1$ and
$\langle \tilde{V}_y \rangle_L$ would exceed $\tilde{V}_T$. This result is consistent with Wang & Maxey's simulation
(1993). However, for very small values of the Stokes number, their results show a very
small increase in the average settling velocity. This can be explained because initially
they located the particles randomly with a uniform distribution and some of them
would have been trapped inside the vortices for a very long time, an effect that is even
stronger when St or V_T are smaller (Perkins & Hunt 1987). For particles without
inertia ($F_p \rightarrow 0$), the result of Maxey & Corrsin (1986) shows that $\langle \tilde{V}_y \rangle_L = \tilde{V}_T$ is
only valid in the limit of $St = 0$, for which some particles released in the vortex core
remain trapped. However, for particles with small inertia, Maxey (1987) showed that
the Lagrangian average settling velocity $\langle \tilde{V}_y \rangle_L$ is always larger than $\tilde{V}_T$.

Using numerical simulations of a three-dimensional random velocity field that
approximates to a turbulent field, Fung (1993) found that $\langle \tilde{V}_y \rangle_B$ is less than $\tilde{V}_T$ over
a limited range of values of F_p and V_T ($> O(1)$). Recently, Ushijima (1998) found
that $\langle \tilde{V}_y \rangle_B$ is 15% greater than $\tilde{V}_T$ for $\tilde{V}_T < \tilde{u}'_y$. We have found that for line vortices,
because D may become positive for a certain range of the parameter F_p, $\langle \tilde{V}_y \rangle_B$ may
be greater as well as less than $\tilde{V}_T$.

Our result is in good agreement with the experimental results of Srdic (1999), who
measured particles settling in turbulence generated by an oscillating grid in a water
tank. He found that $\langle \tilde{V}_y \rangle_L > \tilde{V}_T$ for small values of F_p whereas $\langle \tilde{V}_y \rangle_L < \tilde{V}_T$ for
moderate values of F_p (notice that in his definition of F_p he uses the integral timescale
of turbulence as the characteristic timescale). He found that the maximum average
settling velocity was as much as 80% higher than the particle terminal velocity
and that the maximum reduction was about 20% of the terminal velocity. For very
large values of F_p, the bulk and Lagrangian settling velocity, $\langle \tilde{V}_y \rangle_L$, $\langle \tilde{V}_y \rangle_B$ tended
monotonically towards the terminal velocity $\tilde{V}_T$.

Wang & Maxey (1993, figure 21) showed that $\langle \tilde{V}_y \rangle_L$ increases with the dimensionless
terminal velocity until a maximum is reached for $V_T \sim 1$. Increasing V_T results in an
increase of $F_p = St V_T^2$. Thus, for a small value of St, the bulk settling velocity changes
from being larger to being smaller compared with the terminal velocity of particles.
Srdic (1999) also found this evolution of the average settling velocity as a function of
the dimensionless terminal velocity and he found that $\langle \tilde{V}_y \rangle_L < \tilde{V}_T$ for $\tilde{V}_T > \tilde{u}'_y$ for all
values of F_p.

6.1. *Colliding distance of particle pairs*

The colliding distance of pairs of a large (L) and a small (S) particle in still fluid is $\tilde{l}_0 = (\tilde{V}_T^L - \tilde{V}_T^S)\Delta\tilde{t}$. A similar argument can be derived for particles moving around vortex lines. A particle released at a level $\tilde{Y}_0$ far above the vortex, after falling a time $\Delta\tilde{t} \gg 2\tilde{Y}_0/\tilde{V}_T$ will be at $\tilde{Y} = \tilde{Y}_0 - \tilde{V}_T\Delta\tilde{t} + \Delta\tilde{\eta}$, (see figure 1). Therefore, to arrive at a fixed level $\tilde{Y}_1$, it should be released at $\tilde{Y}_0 = \tilde{Y}_1 + \tilde{V}_T\Delta\tilde{t} - \Delta\tilde{\eta}$, and the colliding distance of particle pairs is

$$\tilde{l} = \tilde{Y}_0^L - \tilde{Y}_0^S = (\tilde{V}_T^L - \tilde{V}_T^S)\Delta\tilde{t} - (\Delta\tilde{\eta}^L - \Delta\tilde{\eta}^S). \tag{6.5}$$

Since $\Delta\tilde{\eta} = (\tilde{\Gamma}/\tilde{V}_T)\Delta\hat{\eta}$,

$$\frac{\langle\tilde{l}\rangle}{\tilde{l}_0} = 1 - \frac{\langle\Delta\tilde{\eta}^L\rangle - \langle\Delta\tilde{\eta}^S\rangle}{(\tilde{V}_T^L - \tilde{V}_T^S)\Delta\tilde{t}} = 1 + \frac{(\tilde{\Gamma}/\tilde{V}_T^S)}{\tilde{V}_T^L\Delta\tilde{t}}\frac{\lambda\langle\Delta\tilde{\eta}^L\rangle - \langle\Delta\tilde{\eta}^S\rangle}{\lambda - 1}, \tag{6.6}$$

where $\lambda = \tilde{V}_T^S/\tilde{V}_T^L$. From (5.3), we obtain

$$\frac{\langle\tilde{l}\rangle}{\tilde{l}_0} = 1 + \frac{(\tilde{\Gamma}/\tilde{V}_T^S)^2}{(\tilde{V}_T^L\Delta\tilde{t})\tilde{L}_x}\left[\frac{\lambda^2 D^L - D^S}{\lambda - 1} + (\lambda + 1)f\left(\frac{\hat{Y}_0}{\hat{L}_x}\right)\right]. \tag{6.7}$$

The highest collision efficiency between particle pairs (cross-section value) is given for similar sizes, i.e. $\lambda \simeq 1$. In these conditions, the maximum $\langle\tilde{l}\rangle/\tilde{l}_0$ is given at $F_p \simeq 0.1$ (see figure 10). In the case of water drops in air with vortices of radius $\tilde{R}_v = 1.5$ mm, this means drops of radius around $20\,\mu$m (with a dimensionless terminal velocity $V_T = \tilde{V}_T/(\tilde{\Gamma}/\tilde{R}_v) = 0.48$). Recent experiments of water droplets in clouds show that this size corresponds to the critical value around which the collision rate has its maximum (Jonas 1996 and references therein).

7. Conclusions and implications of the results

We have studied the behaviour of small heavy particles moving around line vortices. In particular, we have analysed some singular properties of the trajectories in order to understand the physics of the settling of particles and other related problems of interest. We have defined the key dimensionless parameters when the lift and history forces are negligible, to be the particle Froude number F_p and the dimensionless terminal velocity V_T normalized on the peak vertical velocity. By considering these parameters and the trajectories near the particle stagnation point X_P, many of the effects of particle inertia for *any* value of the terminal velocity can be explained. We have included the effect of finite Reynolds number of the particle by using a modified (but linear) Stokes drag law.

When the terminal velocity $\tilde{V}_T$ is less than the maximum vertical velocity of the vortex $\tilde{u}_{y_{max}}$, there exist some regions that the particles cannot reach. For very small values of F_p, these empty regions are narrow bands of width $\tilde{W}_e \propto \tilde{R}_v F_p/V_T$ (see (4.1)). When F_p is of order unity and $V_T \ll 1$, $\tilde{W}_e$ is much larger than $\tilde{R}_v$, the radius of the vortex. In three-dimensional flows with vortices having random orientations, only a few particles would enter these regions, so there would be zones of low particle concentration.

The asymptotic methods presented in §3 are valid for any values of F_p and V_T and any localized two-dimensional or three-dimensional vorticity flows, assuming that the characteristic distance between the vortices is of the order of, or much larger than, $\tilde{\Gamma}/\tilde{V}_T$ when the particles are moving far from the vortex cores. Therefore, it could

be applied to any general type of flow where vorticity is locally concentrated. As figures 5 and 10 show, results using asymptotic analysis give a good approximation to $\tilde{W}_e$ and $\langle\tilde{V}_y\rangle_L$ for $F_p < 0.1$. This concept may possibly be useful for modelling one- and two-particle dispersion (J. C. Vassilicos 1997, private communication) and to simplify numerical codes for two-phase flows.

We have analyzed the phenomenon of 'overshooting', when the trajectory of a particle has an abrupt change in its direction. This is likely to appear near any kind of vortex when F_p is of order unity and in regions where the velocity of the particle is small, i.e. near the equilibrium points of the system for a given fluid velocity field. In the situation where $V_T < 1$, X_P approaches the vortex core as F_p increases. The maximum value of F_p calculated in these cases for the Rankine vortex, F_{p_m}, is of order unity. This is because if the inertia is too large, the particle velocity cannot be reduced to zero before it passes through the vortex core. These concepts are also applicable to dense particles in liquids. Even if $\beta \sim 1$, the motions are largely determined by F_p and V_T.

The bulk settling velocity $\langle\tilde{V}_y\rangle_B$ is always larger than the terminal velocity for small F_p, and V_T less than unity. In this range of V_T, it increases with F_p until a maximum is reached at a certain value $F_{p_M} \sim 1$. Notice that $St \gg 1$ at the maximum $\langle\tilde{V}_y\rangle_B$ if $V_T \ll 1$. For large values of the particle Froude number, $\langle\tilde{V}_y\rangle_B$ is smaller than $\tilde{V}_T$ with a minimum at $F_p = F_{p_m}$ which increases whenever V_T increases. For very large values of F_p, as well as for very large values of the dimensionless terminal velocity, $\langle\tilde{V}_y\rangle_B \to \tilde{V}_T$.

Although these results have been demonstrated only for particles settling near a Rankine vortex the same qualitative results are expected to be valid for many other flows with coherent vortices, because these vortices determine the differential settling. The results may have significant practical application in estimating particle displacements in strongly rotational flows such as centrifuges. In such flows, the vortices of the turbulence tend to be aligned parallel to that of the rotation axis so that the concepts developed here are quite relevant. Our study is restricted to steady flows, but the results can be used to indicate settling behaviour in turbulent flows with intermediate Reynolds numbers if the characteristic time for the deformation of the vortical structures is much larger than the characteristic time of the settling process $\tilde{\Gamma}/\tilde{V}_T^2$. It can be seen from (3.6) that the effect of the unsteadiness appears in the first-order approximation of the small F_p asymptotics. The ratio between this effect and the centrifugal forces is the Strouhal number, $(\tilde{\Gamma}/\tilde{V}_T^2)/\tilde{t}_c$, where $\tilde{t}_c$ is the characteristic time of changes of the flow structures.

Some investigations have suggested that the average settling velocities can be estimated by considering the variation in the concentration of particles in different points of the flow around the vortices. There is certainly a good correlation between concentration of particles and settling velocity when the inertia of the particles is small because for $F_p < 1$ the main effect is the inertial bias of particles towards regions of low vorticity and high strain rate (Squires & Eaton 1991). However, the subtle effects exposed here about the motion of inertial particles near vortices suggest that it is not possible to estimate the averages values of $\tilde{V}_y$ derived from the distribution of particle concentration and on estimates of the local fall speed. One of the reasons is that for particles with large inertia, the overshooting effect described in §4 is much more important. As a result, the correlation between particle concentration and $\langle\tilde{V}_y\rangle_B$ is poor, especially for $F_p > O(1)$.

College Cambridge and from the Technological University of Delft. We are grateful for helpful comments by the referees.

Appendix A. Influence of the particle Reynolds number

An accurate value of the drag force on a spherical rigid particle at moderate and low Reynolds number of the particle, $Re_p = \tilde{d}_p(|\tilde{\boldsymbol{u}} - \tilde{\boldsymbol{V}}|)/\tilde{v}$, where $\tilde{\boldsymbol{u}}$ and $\tilde{\boldsymbol{V}}$ are, respectively, the velocity of the fluid and the particle at the same point, is

$$3\pi f_1 \tilde{d}_p \tilde{\rho}_f \tilde{v}(\tilde{\boldsymbol{u}} - \tilde{\boldsymbol{V}}), \tag{A 1}$$

where $f_1 = 1 + 0.15 Re_p^{2/3}$ (Clift, Grace & Weber 1978). Since $\tilde{\boldsymbol{V}} \simeq \tilde{\boldsymbol{u}} + \tilde{\boldsymbol{V}}_T$ for particles with small inertia (see (3.6)) we linearize f_1 around $\tilde{\boldsymbol{u}} - \tilde{\boldsymbol{V}} = -\tilde{\boldsymbol{V}}_T$,

$$f_1 \simeq k_T + 0.1 Re_T^{2/3}|\hat{\boldsymbol{u}} - \boldsymbol{j} - \hat{\boldsymbol{V}}|, \tag{A 2}$$

where $k_T = 1 + 0.15 Re_T^{2/3}$ and, as a result of scaling the velocities with $\tilde{V}_T$, we have defined the terminal Reynolds number of the particle $Re_T = \tilde{d}_p \tilde{V}_T/\tilde{v}$. Thus, $f_1 \simeq k_T$ is a good approximation if

$$Re_T < 1. \tag{A 3}$$

In this way, the linear drag law can be extended to consider the influence of the particle Reynolds number.

Appendix B. Bulk settling velocity for particles with large V_T

Consider a particle with settling velocity $\tilde{\boldsymbol{V}}_T = (0, -\tilde{V}_T)$ in still fluid, moving in a velocity field having a vertical velocity $\tilde{u}_y(\tilde{\boldsymbol{x}}, \tilde{t})$ with $\langle \tilde{u}_y \rangle_E = 0$, r.m.s. value $\tilde{u}_y'$ and integral scale $\tilde{L}$. Consider the limiting situation where $\tilde{V}_T \gg \tilde{u}_y'$ so that from (3.6) the vertical velocity of the particle

$$\tilde{V}_y = \tilde{u}_y(\tilde{X}, \tilde{t}) - \tilde{V}_T, \tag{B 1}$$

where $\mathrm{d}\tilde{X}/\mathrm{d}\tilde{t} = \tilde{V}$. The error in this approximation is $\tilde{t}_p \, \mathrm{d}\tilde{V}_y/\mathrm{d}\tilde{t} \simeq -\tilde{t}_p \tilde{V}_T \partial \tilde{u}_y/\partial \tilde{y}$, which tends to zero as St or $F_p \to 0$. The settling time $\Delta \tilde{T}$ between levels $\tilde{Y}_0$ and $\tilde{Y}_1$, where $\tilde{Y}_0 - \tilde{Y}_1 \gg \tilde{L}$, is given by

$$\Delta \tilde{T} = \int_{\tilde{Y}_0}^{\tilde{Y}_1} \frac{\mathrm{d}\tilde{Y}}{\tilde{u}_y - \tilde{V}_T} = \frac{\tilde{Y}_0 - \tilde{Y}_1}{\tilde{V}_T} + \int_{\tilde{Y}_1}^{\tilde{Y}_0} \frac{\tilde{u}_y}{\tilde{V}_T^2} \, \mathrm{d}\tilde{Y} + \int_{\tilde{Y}_1}^{\tilde{Y}_0} \frac{\tilde{u}_y^2}{\tilde{V}_T^3} \, \mathrm{d}\tilde{Y} + \cdots, \tag{B 2}$$

if $\overline{(\tilde{u}_y)}_E = 0$,

$$\langle \Delta \tilde{T} \rangle = \frac{\tilde{Y}_0 - \tilde{Y}_1}{\tilde{V}_T} \left(1 + \frac{\overline{(\tilde{u}_y^2)}_E}{\tilde{V}_T^2} + \cdots \right).$$

Thence, from its definition, the bulk settling velocity

$$\langle \tilde{V}_y \rangle_B = \frac{\tilde{Y}_0 - \tilde{Y}_1}{\langle \Delta \tilde{T} \rangle} = \tilde{V}_T \left(1 - \frac{\overline{(\tilde{u}_y^2)}_E}{\tilde{V}_T^2} + \cdots \right) < \tilde{V}_T. \tag{B 3}$$

This is qualitatively consistent with the results of §§5 and 6 in that if the particle distribution is uniform, the spatial average of $\tilde{u}_y$ over all particles is equal to $\langle \tilde{u}_y \rangle_E$. Hence from (B 1), $\langle -\tilde{V}_y \rangle_E = \tilde{V}_T$ since $\langle \tilde{u}_y \rangle_E = 0$. Notice also that if $V_T < 1$, regions

with positive contribution to $\langle\tilde{u}_y\rangle_L$ disappear from the integrals and as a result $\langle\tilde{u}_y\rangle_L < 0$. Note also that in the case of a line vortex where $\tilde{Y}_1 = -\tilde{Y}_0$,

$$\int_{\tilde{Y}_1}^{\tilde{Y}_0}\langle\tilde{u}_y\rangle\,\mathrm{d}\tilde{Y} = 0, \qquad \int_{\tilde{Y}_1}^{\tilde{Y}_0}\langle\tilde{u}_y^2\rangle\,\mathrm{d}\tilde{Y} = A(\tilde{\Gamma}^2/\tilde{R}_v) > 0,$$

where A is a coefficient of order unity. Therefore, for our particular case,

$$\Delta\tilde{T} = \frac{\tilde{Y}_0 - \tilde{Y}_1}{\tilde{V}_T} + A\frac{(\tilde{\Gamma}^2/\tilde{R}_v)}{\tilde{V}_T^3}, \tag{B 4}$$

and from its definition

$$\langle\tilde{V}_y\rangle_B \simeq \tilde{V}_T\left[1 - A\frac{\tilde{\Gamma}^2/\tilde{R}_v}{(\tilde{Y}_0 - \tilde{Y}_1)\tilde{V}_T^2}\right] = \tilde{V}_T\left[1 - A\frac{\tilde{R}_v}{(\tilde{Y}_0 - \tilde{Y}_1)}\frac{\tilde{U}^2}{\tilde{V}_T^2}\right], \tag{B 5}$$

shows how particles which cut trough the eddies have a lower bulk settling velocity.

REFERENCES

CHEIN, R. & CHUNG, J. N. 1987 Effects of vortex pairing on particle dispersion in turbulent shear flows. *Intl J. Multiphase Flow* **13**, 785–802.

CLIFT, R., GRACE, J. R. & WEBER, M. E. 1978 *Bubbles, Drops and Particles.* Academic.

FERNÁNDEZ-FERIA, R., FERNÁNDEZ DE LA MORA, J. & BARRERO, A. 1995 Solution breakdown in a family of self-similar nearly inviscid axisymetric vortices. *J. Fluid Mech.* **305**, 77–91.

FUNG, J. C. H. 1993 Gravitational settling of particles and bubbles in homogeneous turbulence. *J. Geophys. Res.* **98**, 20 287–20 297.

GAÑÁN-CALVO, A. M. & LASHERAS, J. C. 1991 On the dynamics of small spherical particles in a shear layer. *Phys. Fluids* A **3**, 1207–1217.

HUNT, J. C. R., PERKINS, R. & FUNG, J. C. H. 1994 Problems in modeling disperse two-phase flows. *Appl. Mech. Rev.* **47**, S49–S60.

JIMÉNEZ, J., WRAY, A. A., SAFFMAN, P. G. & ROGALLO, R. S. 1993 The structure of intense vorticity in isotropic turbulence. *J. Fluid Mech.* **255**, 65–90.

JONAS, P. R. 1996 Turbulence and clouds microphysics. *Atmos. Res.* **40**, 283–306.

KOWE, R., HUNT, J. R. C., HUNT, A., COUET, B. & BRADBURY, L. S. J. 1988 The effect of bubbles on the volume fluxes and the pressure gradients in non-uniform steady flow of liquids. *Intl J. Multiphase Flow* **14**, 587–606.

LASHERAS, J. C. & TIO, K. K. 1994 Dynamics of a small spherical particle in steady two-dimensional vortex flows. *Appl. Mech. Rev.* **47**, S61–S69.

MCLAUGHLIN, J. B. 1988 Particle size effects on Lagrangian turbulence. *Phys. Fluids* **31**, 2544–2553.

MAGNAUDET, J. & EAMES, I. 2000 The motion of high-Reynolds-number bubbles in inhomogeneous flows. *Ann. Rev. Fluid Mech.* **32**, 659–708.

MARCU, B., MEIBURG, E. & NEWTON, P. K. 1995 Dynamics of heavy particles in a Burgers vortex. *Phys. Fluids* **7**, 400–410.

MARTIN, J. E. & MEIBURG, E. 1994 The accumulation and dispersion of heavy particles in forced two-dimensional mixing layers. I. The fundamental and subharmonic cases. *Phys. Fluids* **6**, 1116–1132.

MAXEY, M. R. 1987 The gravitational settling of aerosol particles in homogeneous turbulence and random flow fields. *J. Fluid Mech.* **174**, 441–465.

MAXEY, M. R. & CORRSIN, S. 1986 Gravitational settling of aerosol particles in randomly orientated cellular flow fields. *J. Atmos. Sci.* **43**, 1112–1134.

MAXEY, M. R. & RILEY, J. J. 1983 Equation of motion for a small rigid sphere in a nonuniform flow. *Phys. Fluids* **26**, 883–889.

PERKINS, R. & HUNT, J. C. R. 1987 Particle transport in turbulent shear flows. Unpublished. Report to SERC (available from J.C.R.H.).

PERKINS, R., GHOSH, S. & PHILLIPS, J. C. 1991 The interaction between particles and coherent

structures in a plane turbulent jet. *Advances in Turbulence III* (ed. A. V. Johansson & P. H. Alfredsson). Springer.

PRESS, W. H., TEUKOLSKY, S. A., VETTERING, W. T. & FLANNERY, B. P. 1992 *Numerical Recipes in C. The Art of Scientific Computing.* Cambridge University Press.

RAJU, N. & MEIBURG, E. 1995 The accumulation and dispersion of heavy particles in forced two-dimensional mixing layers. Part 2. The effect of gravity. *Phys. Fluids* **7**, 1241–1264.

RAJU, N. & MEIBURG, E. 1997 Dynamics of small spherical particles in vortical and stagnation point flow fields. *Phys. Fluids* **9**, 299–314.

SQUIRES, K. D. & EATON, J. K. 1991 Preferential concentration of particles by turbulence. *Phys. Fluids* A **3**, 1169–1178.

SRDIC, A. 1999 Interaction of dense particles with stratified and turbulent environments. PhD thesis, Arizona State University.

USHIJIMA, T. 1998 The motion of heavy particles in turbulent flows. PhD thesis, Technological University of Delft.

VINCENT, A. & MENEGUZZI, M. 1994 The dynamics of vorticity tubes in homogeneous turbulence. *J. Fluid Mech.* **258**, 245–254.

WANG, L.-P. & MAXEY, M. R. 1993 Settling velocity and concentration distribution of heavy particles in homogeneous isotropic turbulence. *J. Fluid Mech.* **256**, 27–68.

WANG, L-P. & STOCK, D. E. 1993 Dispersion of heavy particles by turbulent motion. *J. Atmos. Sci.* **50**, 1897–1913.

WEN, F., KAMALU, N., CHUNG, J. N., CROWE, C. T. & TROUTT, T. R. 1992 Particle dispersion by vortex structures in plane mixing layers. *Trans. ASME: J. Fluids Engng* **114**, 657–666.